Received: 10 June 2020 | Revised: 17 December 2020 | Accepted: 21 December 2020

DOI: 10.1111/jmg.12591

ORIGINAL ARTICLE

Journal of METAMORPHIC GEOLOGY WILEY

Diachronous collision in the Seve Nappe Complex: Evidence from Lu–Hf geochronology of eclogites (Norrbotten, North Sweden)

Kathrin Fassmer[1,2] | Nikolaus Froitzheim[1] | Marian Janák[3] | Merle Strohmeyer[1] | Michał Bukała[4,5] | Markus Lagos[1] | Carsten Münker[6]

[1]Institute of Geosciences, University of Bonn, Bonn, Germany

[2]Department of Geology, University of Innsbruck, Innsbruck, Austria

[3]Earth Science Institute, Slovak Academy of Sciences, Bratislava, Slovak Republic

[4]Faculty of Geology, Geophysics and Environmental Protection, AGH University of Science and Technology, Kraków, Poland

[5]Instituto Andaluz de Ciencias de la Tierra, CSIC & Universidad de Granada, Granada, Armilla, Spain

[6]Institute of Geology and Mineralogy, University of Cologne, Cologne, Germany

Correspondence
Kathrin Fassmer, Institute of Geosciences, University of Bonn, Bonn, Germany.
Email: kathrin.fassmer@uibk.ac.at

Funding information
Agentúra na Podporu Výskumu a Vývoja, Grant/Award Number: APVV-18-0107; Deutsche Forschungsgemeinschaft, Grant/Award Number: FR700/18-1

Handling Editor: Dr. Julia Baldwin

Abstract

The collision of Baltica and Laurentia during the Caledonian Orogeny happened at *c*. 400–420 Ma. However, subduction and collision processes also took place before this main collisional phase and the tectonic history of these is still not fully resolved. The Seve Nappe Complex in Sweden has recorded these earlier phases. The Seve Nappe Complex in Norrbotten (North Swedish Caledonides) comprises four superimposed nappes emplaced by eastward thrusting (from base to top according to the conventional structural interpretation): Lower Seve Nappe, Vaimok, Sarek, and Tsäkkok Lenses. Eclogites occur in the Vaimok and Tsäkkok Lenses. The Vaimok Lens represents rocks of the Baltican continental margin intruded by Neoproterozoic dolerite dikes which were later eclogitized and boudinaged. By contrast, eclogites of the Tsäkkok Lens are former oceanic basalts associated with calcschists, possibly representing the ocean–continent transition between Baltica and Iapetus. Previous age determinations for eclogitization yielded various ages between *c*. 500 and 480 Ma, in contrast to younger (460–450 Ma) ages of ultra high-*P* metamorphism in the Seve Nappe Complex further south in Jämtland. Eclogites from the Vaimok (one sample) and Tsäkkok (three samples) lenses were dated using Lu–Hf garnet geochronology. Garnet from all samples shows prograde zoning of major element and Lu contents and yielded well-defined isochrons of the following ages: 480.4 ± 1.2 Ma (Vaimok); 487.7 ± 4.6 Ma, 486.2 ± 3.2, 484.6 ± 4.6 Ma (Tsäkkok). The ages from Tsäkkok are interpreted to date the burial of the Iapetus–Baltica ocean–continent transition in a west-dipping subduction zone around *c*. 485 Ma, and the age from the structurally deeper Vaimok Nappe the following subduction of the continental margin. Previously reported ages of 500 Ma and older are not supported by this study. The age difference between eclogites in the Seve Nappe Complex in Jämtland (*c*. 460–450 Ma) and Norrbotten (*c*. 488–480 Ma) may reflect the collision of an island arc with an irregularly shaped passive continental margin of Baltica or alternatively the collision of a straight margin with a microcontinent (Sarek Lens) accreted to the upper plate.

KEYWORDS

Caledonian Orogeny, garnet, high-*P* metamorphism, Lu–Hf geochronology, Seve Nappe Complex

1 | INTRODUCTION

Research in mountain belts worldwide has shown that continental crust is subducted during collisional orogeny, opposing the classical concept that continental crust is not subducted and post-collisional convergence is accommodated by thickening of the lithosphere only (e.g. Gilotti, 2013; Hacker & Gerya, 2013). Tectonic and geophysical observations have shown that continental lithosphere in different ancient and active collision zones is indeed subducted down to mantle depths but mechanisms for continental subduction and exhumation are still incompletely understood. This is also the case for the Himalaya–Tibet collisional system, the main site of research into the deformation of continents, subduction of continental crust, and the feedback between tectonics, erosion, and atmospheric circulation (e.g. Liou et al., 2004). As the tectonic processes occurring in the deeper levels of this orogen are not directly accessible, it is useful to study a similar collisional orogen where the deep levels are exposed. A suitable study area is the *c*. 400–500 Ma old, deeply eroded Caledonian Orogen of Scandinavia, where continental subduction occurred in the Early Palaeozoic due to the collision of the continents Baltica and Laurentia (e.g. Brueckner & Van Roermund, 2007; Cutts & Smit, 2018; Hacker et al., 2010; Kylander-Clark et al., 2009; Root & Corfu, 2012). The Seve Nappe Complex, which experienced ultra high pressure (UHP) metamorphism before the main collision, is an ideal location to study the early evolution of the Caledonian orogeny. Ages for UHP metamorphism, especially in Norrbotten, are still not fully constrained and vary between *c*. 480 and *c*. 505 Ma, depending on the dating method used (Mørk et al., 1988; Root & Corfu, 2012). As age investigations are essential for reconstructing the tectonic evolution of this part of the orogen, we subjected garnet from Norrbotten eclogites to Lu–Hf geochronology. This approach has the potential to precisely and accurately date the (re-)crystallization of garnet, a mineral that grows during increasing pressure (subduction; e.g. Baxter & Scherer, 2013; Lapen et al., 2003). As Lu–Hf garnet ages for an eclogite from the Seve nappe in southern Jämtland were already obtained (Fassmer et al., 2017), the new data will allow us to assess lateral diachroneity of eclogitization within this important thrust unit and therefore will help to improve the tectonic models for early Caledonian HP metamorphism.

2 | GEOLOGICAL SETTING

2.1 | Scandinavian Caledonides

The Scandian mountains expose an up to 300 km wide and 1,500 km long lower to middle crustal section through a Himalayan-type orogen. Towards the west, locally derived nappes are overridden by successively more far-transported units (Gee et al., 2008). The thrust sheets have a small vertical thickness in comparison to their vast areal extent. Generally, thrust units were emplaced east- to southeastwards and the resulting edifice was overprinted by mostly west- to northwest-dipping extensional faults and large-scale open bending (Corfu et al., 2014; Fossen, 2000). The thrust units rest on parautochthonous Baltican basement which is exposed in windows at the Norwegian coast, the biggest one being the Western Gneiss Complex. The far-travelled thrust nappes have been grouped into four allochthons: Lower, Middle, Upper, and Uppermost (Gee et al., 1985; Roberts & Gee, 1985; Figure 1). The Lower Allochthon is interpreted to be derived from the Baltoscandian platform and includes a rifted margin and foreland basins. It seems to be the only unit that is almost certainly free of Palaeozoic HP/UHP rocks (Brueckner & van Roermund, 2004). The Middle Allochthon consists of the outer and outermost margin of Baltica and the continent–ocean transition zone. The Upper Allochthon comprises terranes of primarily oceanic affinity (ophiolites, island-arc magmatic complexes, forearc basins), some derived from proximal to Laurentia, and some to Baltica (Gale & Roberts, 1974; Pedersen et al., 1991; Stephens & Gee, 1985). The Uppermost Allochthon contains fragments of the outer margin of Laurentia and terranes that were accreted to this margin during the closure of the Iapetus Ocean (Krogh et al., 1990; Pedersen et al., 1992; Stephens & Gee, 1985, 1989).

High-*P* metamorphism related to the Caledonian Orogeny occurred in several episodes of time (*c*. 480–500 Ma, *c*. 450–460 Ma, *c*. 400–420 Ma), which are either partly connected or represent separate events of subduction of continental crust. The last episode is related to the final collision of Baltica and Laurentia and is referred to as the Scandian Orogeny (e.g. Robert, 2003). Scandian HP/UHP metamorphism is found in the Western Gneiss Region (e.g. Carswell et al., 2003; Cutts & Smit, 2018; Kylander-Clark et al., 2007; Root et al., 2004) and in Lofoten (Froitzheim et al., 2016), which are parts of the Baltican margin that was subducted under Laurentia during the continent collision. Older UHP metamorphism can be found in different parts of the Caledonian nappe stack. One location is the Jæren Nappe in SW Norway, where eclogite facies metamorphism was dated to *c*. 470 Ma. This unit was interpreted to be derived from the Taconian collision zone at the Laurentian margin (Smit et al., 2010, 2011). *C*. 450 Ma old UHP metamorphism was found in the Tromsø Nappe of the Uppermost Allochthon (Fassmer et al., 2020; Janák et al., 2012; Janák, Ravna, et al., 2013; Ravna & Roux, 2006). This unit is mostly also interpreted to be derived from the Taconian collision zone (Corfu et al., 2003). However, similar ages (460–450 Ma) for UHP metamorphism were also reported in the Seve Nappe Complex in Jämtland, interpreted as a part of the distal Baltican margin (Brueckner & Van

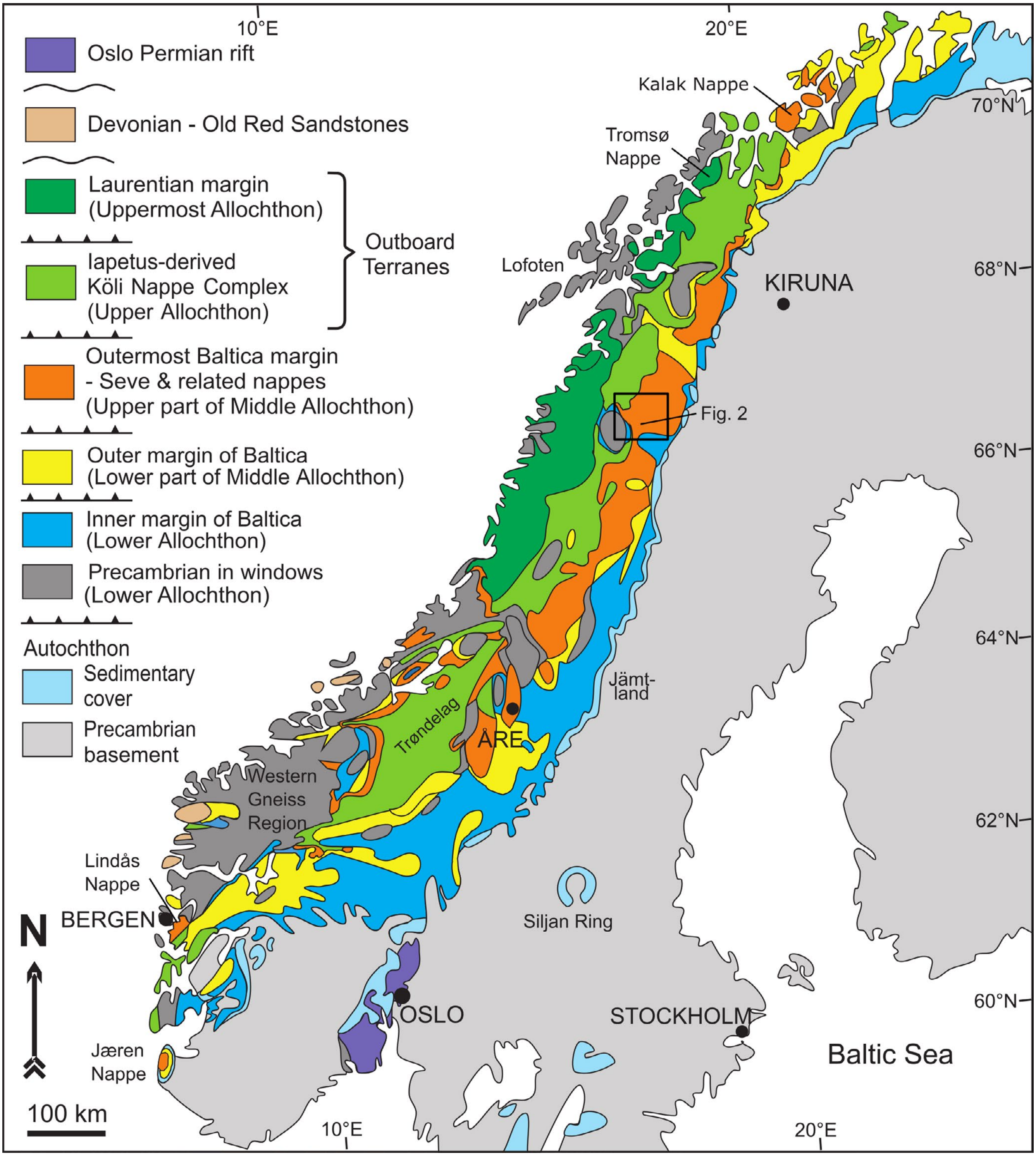

FIGURE 1 Tectonostratigraphic map of the Scandinavian Caledonides after Gee et al. (2010). The black square marks the study area

Roermund, 2007; Fassmer et al., 2017; Grimmer et al., 2015; Root & Corfu, 2012). Therefore, Janák et al. (2012) suggested that the Tromsø Nappe may not come from Laurentia but instead represents a part of the (Baltican) Seve Nappe Complex that was emplaced by out-of-sequence thrusting on top of the nappe edifice during Scandian collision. The Seve Nappe Complex has classically been interpreted to represent the ocean–continent transition between Baltica and the Iapetus Ocean (Andréasson, 1986, 1994; Andréasson et al., 1998), but some authors also interpret the Seve Nappe Complex as being exotic to Baltica (e.g. Corfu et al., 2007; Kirkland et al., 2006). A further complication arises from the eclogites of the Seve Nappe Complex in Norrbotten, located between Jämtland and Tromsø, which have yielded various *c*. 500 Ma (e.g. Mørk et al., 1988) to 480 Ma (e.g. Root & Corfu, 2012) ages. These are the subject of the present work. In general, early Caledonian ages (*c*. 500–450 Ma) in the Seve Nappe Complex were ascribed to arc–continent collision and possibly microcontinent collision preceding the Scandian continent–continent collision (Brueckner & Van Roermund, 2007).

2.2 | The Seve Nappe Complex

The Seve Nappe Complex is part of the Middle Allochthon and can be followed at least 1,000 km along the length of the Scandinavian Caledonides. In this nappe complex and the underlying Särv Nappe (lower metamorphic grade) swarms of dolerite dykes occur. These are interpreted as being part of a larger igneous province (Albrecht, 2000), which is related to Iapetan rifting. Intrusion ages of these dykes are *c*. 607–619 Ma (e.g. Svenningsen, 2001). Similar ages of *c*. 615–550 Ma are constrained for dykes at the Appalachian margin (e.g. Soper, 1994). Caledonian HP to UHP rocks are found in the Seve Nappe Complex in Jämtland (Janák et al., 2013; Klonowska et al., 2016, 2017; Majka et al., 2014), Västerbotten (Bukała, Majka, et al., 2020; Petrík et al., 2019), and Norrbotten (Bukała et al., 2018). Ages of this UHP metamorphism are between 445 and 500 Ma (e.g. Brueckner & Van Roermund, 2007; Fassmer et al., 2017; Mørk et al., 1988).

2.3 | Norrbotten

The Seve Nappe Complex in Norrbotten is traditionally subdivided into three megalenses which are from bottom to top: Vaimok Lens, Sarek Lens, and Tsäkkok Lens (Albrecht, 2000; Kullerud et al., 1990; Zachrisson & Stephens, 1984; Figure 2). Note, however, that a different stacking order has recently been proposed (Andréasson, 2020; see below). While the Sarek Lens is eclogite free, the two others contain eclogite (Albrecht, 2000; Andréasson & Albrecht, 1995; Kullerud et al., 1990). Below these megalenses there is a thin and discontinuous nappe, that is also eclogite free (Lower Seve Nappe). Andréasson (2020) proposed a new tectonic interpretation according to which the nappe stack has been modified by folding. In this interpretation, the Sarek Lens is structurally higher than both the Vaimok and the Tsäkkok lenses. The latter two lenses occupy a similar structural level and may represent one and the same high-*P* terrane. Andréasson also proposed new names for the units. We will use the old, well-introduced names; the new ones can be found in Andréasson (2020).

The Lower Seve Nappe comprises marble, quartzite, amphibolite, and mica schist and the metamorphic grade does not exceed lower amphibolite facies (Albrecht, 2000). The Vaimok Lens consists of quartzite, mica schist, marble, calc–silicate gneiss, metavolcanic rocks, and eclogite. In this nappe, eclogitization was locally incomplete, resulting in boudins of coronitic diabase or only partially eclogitized diabase (Andréasson & Albrecht, 1995). The occurrence of coronitic diabase is restricted to one well-defined area on the southern slope of Mt. Grapesvare, and there is no lithological or structural break in the host rock between eclogite- and diabase-bearing rocks (Albrecht, 2000). The eclogites in the structurally higher parts of the Vaimok Lens occur as boudins in a size range from few decimeters to 25 m and are retrogressed to different degrees, often with foliated amphibolite selvages. Boudins occurring in marble are generally less retrogressed than those in the mica schists and quartzites (Albrecht, 2000). The protoliths of the eclogites are tholeiitic dolerite dykes that intruded the sedimentary sequence prior to Caledonian thrusting and metamorphism (Mørk et al., 1988). Protolith ages of this dyke swarm are *c*. 590–610 Ma (Albrecht, 2000; Barnes et al., 2018; Root & Corfu, 2012; Svenningsen, 2001). Boudins of coronitic diabase are in general larger than eclogite boudins, and the transition to eclogite is well displayed in partially eclogitized diabase boudins. The access and/or composition of fluids may have been the critical factor, either catalysing or inhibiting eclogitization (Albrecht, 2000). Metamorphic conditions in the Vaimok Lens were constrained to 15–27 kbar and 610–750°C by Albrecht (2000), while Bukała et al. (2018) obtained UHP conditions of 28–31 kbar at 660–780°C. Essex et al. (1997) dated the metamorphism of a calc–silicate gneiss in this nappe to 475–500 Ma with U–Pb geochronology on titanites. Metamorphism in eclogites was dated at 503 $\pm$ 14 Ma with Sm–Nd on garnet and omphacite (Mørk et al., 1988) and to 481.9 $\pm$ 1.0 Ma with U–Pb on zircon (Root & Corfu, 2012). Barnes et al. (2018) reported prograde metamorphism with U–Pb–Th on monazite at 498 $\pm$ 10 Ma. The formation of regional foliation is constrained to 491 $\pm$ 8 Ma obtained from Ar–Ar geochronology on hornblende, defining the foliated selvages of eclogite boudins (Dallmeyer & Gee, 1986).

The Sarek Lens, to a large part, consists of mafic dykes that were metamorphosed under amphibolite facies conditions (Svenningsen, 2001). These dykes intruded into a 4–5 km thick succession of rift-related metasediments comprising marble, graphitic dolomite, micaschist, phyllite, and quarzite (Kjøll et al., 2019; Svenningsen, 2001).

The Tsäkkok Lens can be further divided into two lithologically distinct parts, which were referred to as Upper and Lower Tsäkkok by Kullerud et al. (1990). The lower part consists mainly of quartzofeldspathic schist with minor eclogites, amphibolites, and marble while the upper part consists of marble, quartzite, and phengite schist, with abundant eclogite and amphibolite. It also contains glaucophane-bearing eclogitized pillow basalts in a matrix of calcschist in

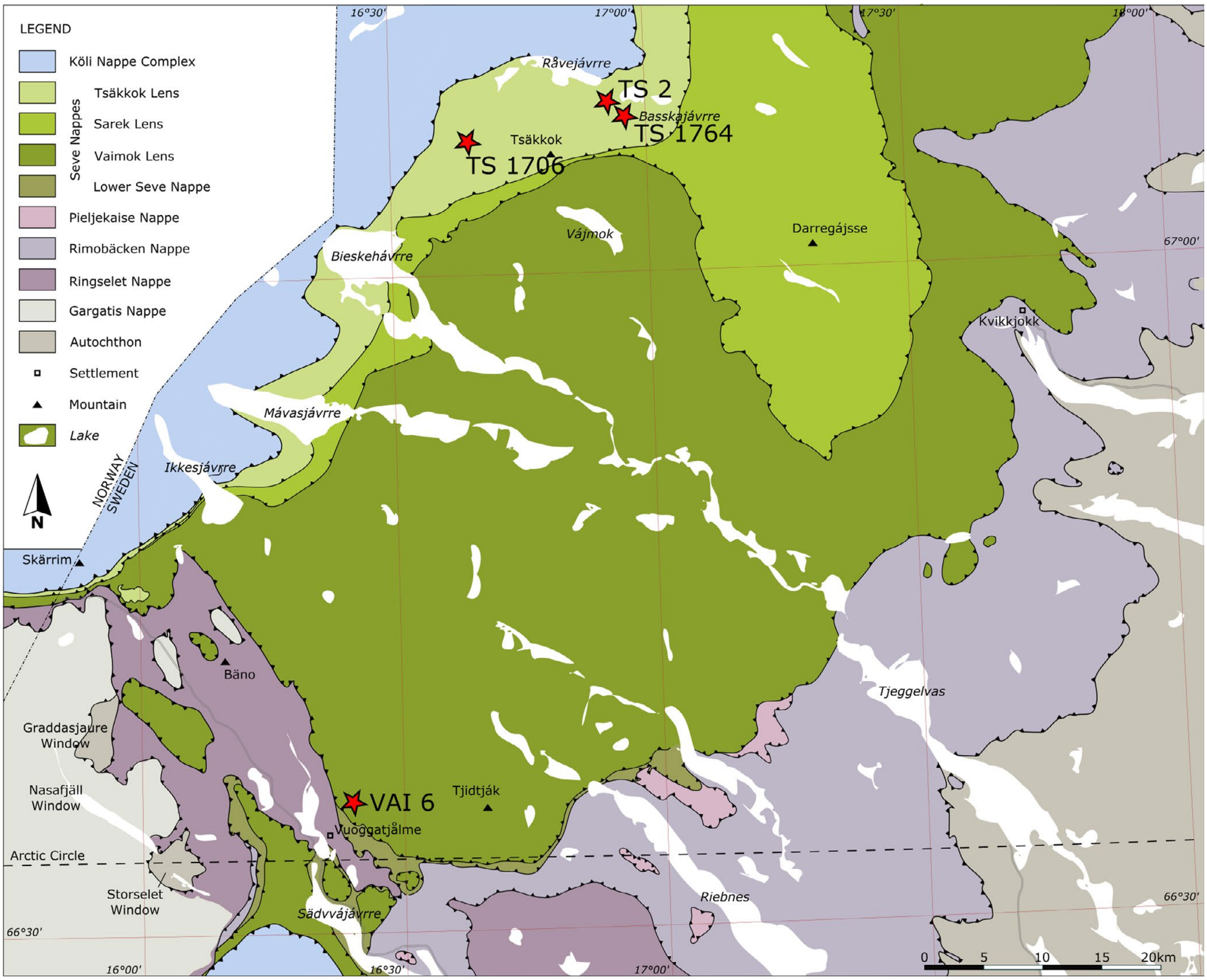

FIGURE 2 Geological map from the Norrbotten region with red stars marking the samples of this study. The map is compiled after Albrecht (2000), Kullerud & Snilsberg (1987) and the bedrock map of the Swedish Geological Survey.

its upper part (Kullerud et al., 1990). There is widespread evidence for a substantially colder metamorphic history than in the Vaimok Lens and pressure and temperature conditions of peak metamorphism were constrained to 500–630°C and 12–15 kbar (Stephens & van Roermund, 1984). This estimate has been somewhat confirmed by Bukała, Barnes, et al. (2020) reporting a brittle deformation of Tsäkkok eclogites in alike temperature, but pressure up to 25 kbar. Mørk et al. (1988) dated this metamorphism at 503 ± 18 Ma with Sm–Nd geochronology, while Root and Corfu (2012) dated it with U–Pb geochronology on zircon at 481.9 ± 1.2 Ma.

The ages obtained for the Seve Nappe Complex in Norrbotten partly fall into the Finnmarkian Orogeny, a major orogenic event that is believed to have affected much of the Northern Scandinavian Caledonides between 520 and 500 Ma (e.g. Roberts, 2003; Sturt et al., 1978). Initially, the Finnmarkian Orogeny was interpreted as an arc–continent collision in which the arc overrode the thinned western edge of Baltica (Andréasson, 1994; Dallmeyer, 1988; Dallmeyer & Gee, 1986; Stephens & Gee, 1985, 1989). Brueckner and van Roermund (2004) have proposed that the arc collided with a microcontinent or peninsula that previously drifted away from Baltica, although the precise timing of this collision remains uncertain. The Vaimok and Tsäkkok Lenses have been subjected to different pressure and temperature conditions, and it was suggested that the Vaimok Lens was subducted to deeper levels than the Tsäkkok Lens (Mørk et al., 1988). These authors interpreted that eclogitization in the two lenses is related to the same high-*P* event but depending on spatial relations and the evolution of the subduction zone, maximum pressures may have been reached at slightly different time.

Field relations in Norrbotten seem remarkably similar to those further south in Jämtland, and the two areas were sometimes considered together (i.e. van Roermund, 1985).

Similarities between Norrbotten and Jämtland seem to reflect nearly identical processes at different times (*c*. 460 Ma in Jämtland and *c*. 480–500 Ma in Norrbotten; Brueckner & van Roermund, 2004). Recently, the spatial and temporal gap in metamorphism between Norrbotten and Jämtland localities has been studied by Petrik et al. (2019). These authors report a U–Th–Pb monazite age of *c*. 472 Ma from a diamond-bearing paragneiss in Saxnäs (southern Västerbotten). While the age of 472 Ma has been interpreted as related to monazite growth under near-peak UHP conditions, Bukała, Majka, et al. (2020) report a zircon U–Pb age of *c*. 473 Ma, interpreted to date the exhumation-related migmatization of garnet amphibolites and host paragneisses from Kittelfjäll (central Västerbotten).

For this study, four eclogite samples were collected (one from the Vaimok and three from the Tsäkkok Lens) and prograde metamorphism dated with Lu–Hf geochronology to constrain the age of subduction in Norrbotten and to compare it to other parts of the Seve Nappe Complex, which will contribute to the understanding of the evolution of the early Caledonian Orogeny. In the Vaimok Lens, samples from a variety of eclogite locations were taken, but because of strong retrograde overprint, only one was suitable for dating. In the Vaimok Nappe most of the (retro-) eclogites occur as metamorphosed dykes of different sizes within metasediment host rock (Figure 3). The three samples from the Tsäkkok Nappe were taken from the area shown in Figure 2. Although a limited amount of samples was taken, three eclogites were suitable for dating. Some of the eclogites in the Tsäkkok Nappe show pillow structures (Figure 3). Unfortunately, we did not find them to be suitable for dating. Therefore, we dated samples that occur as massive lenses in the metasediment host rock.

3 | ANALYTICAL METHODS

Mineral compositions were determined from thin sections using a JEOL Superprobe JXA 8200 electron microprobe,

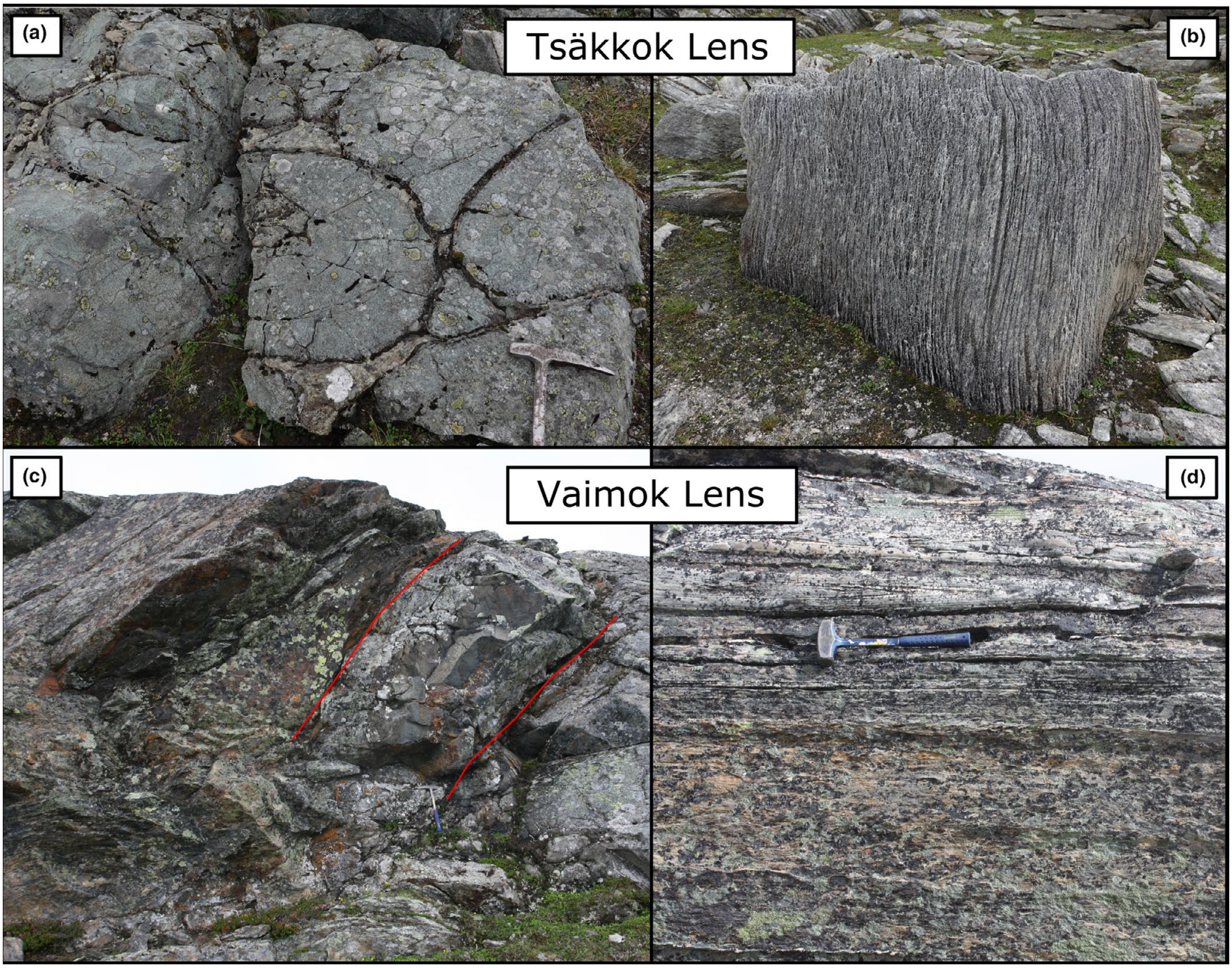

FIGURE 3 Field photographs of (a) eclogitized pillow basalts, (b) calcschist surrounding the eclogites, (c) eclogitized dolerite dyke (between red lines), and (d) garnet-bearing micaschist as host rock of the dyke

situated at the Institute of Geosciences (University of Bonn). Quantitative point analyses were executed in wavelength dispersive mode (WDS) with a beam current of 15 nA and an acceleration voltage of 15 kV. For each measurement point, Si, Ti, Al, Fe, Mn, Mg, Ca, Na, K, and Cr were analysed. Calibration of count rates was carried out with well-defined natural minerals and pure metal alloys: Fe—magnetite, Mg—olivine, Ca—anorthite, Na—scapolite, Si/Al—garnet, K—sanidine, Ti—rutile, Cr—chromium metal, Mn—manganese/iron metal (Jarosewich et al., 1980). The results are given as wt% of the element oxides with Fe given as FeO. Profiles through garnet grains were measured by analysis of points at distances of ~30 μm. If minerals were extraordinarily small or large, the distance was adjusted accordingly. For representative garnet grains, major element (Mg, Fe, Ca, and Mn) distribution maps were also measured. The size of the map and the size of each pixel were chosen manually for each map, to achieve an ideal relation between resolution and measurement time.

Bulk rock chemistry was obtained from whole-rock powders by X-ray fluorescence analysis, using a PANanalytical Axios instrument situated at the Institute of Geosciences (University of Bonn). The following major element oxides were analysed: SiO_2, Al_2O_3, Fe_2O_3, MnO, MgO, CaO, Na_2O, K_2O, TiO_2, P_2O_5.

In addition to the major element distribution in garnet grains, Y, Nd, Sm, Lu, and Hf profiles through the same garnet grains as measured with electron microprobe were also measured. The measurements were undertaken with a Resonetics M50 Excimer 193 nm laser system, connected with a Thermo Scientific Element XR/2 Sector-Field-ICPMS, situated at the Institute of Geosciences (University of Bonn). Measured points for laser ablation were chosen manually to avoid inclusions. The sizes of the laser spots were 58 μm for the sample from the Vaimok Lens and 44 μm for all Tsäkkok samples. The laser fluency at the sample surface was 7 J/cm^2 and the laser repetition rate was set to 10 Hz. In addition to the Y, Nd, Sm, Lu, and Hf, also Si, Mn, Ti, and Zr were measured to monitor possible inclusions. The count rates were measured for 30 s on the gas background and 30 s on each spot with laser on. The count rates were then normalized using ^{29}Si as an internal standard. Calibration was carried out using NIST SRM 612 as an external standard (Jochum et al., 2011) and was measured several times between the samples. Normalized count rates were then converted to concentrations using the procedure after Longerich et al. (1996).

Sample preparation, digestion, and MC-ICPMS measurements for Lu–Hf geochronology were conducted as described in detail by Fassmer et al. (2017). Four garnet separates, one clinopyroxene separate, and two to three whole-rock splits, one digested in a Parr bomb and one or two with the tabletop procedure after Münker et al. (2001) and Lagos et al. (2007), were analysed for each sample. We digested whole-rock splits with both methods to test if zircon or rutile were inherited or grew during the same metamorphic process.

4 | RESULTS

4.1 | EPMA and XRF analyses

Eclogite sample VAI 6 (Vaimok Nappe, N 66°35.803′/E 16°24.328′) has a typical basaltic composition (Table 1). The high-*P* assemblage comprises 35 vol.% garnet, 45 vol.% omphacite, 5 vol.% quartz, calcite, rutile (together 5 vol.%), and accessory ore minerals which can be locally as large as garnet grains. Almost 10 vol.% of the rock consists of symplectites of Na-poor clinopyroxene and plagioclase. Representative electron microprobe analyses of the most important minerals are shown in Table 2.

Garnet porphyroblasts are surrounded mostly by omphacite, which is party replaced by symplectites of Na-poor clinopyroxene with amphibole and plagioclase. Garnet is 0.2–1.5 mm large, mostly xenoblastic to hypidioblastic, and has a composition of $Alm_{48\text{-}56}Gr_{28\text{-}39}Py_{7\text{-}19}Sps_{0.7\text{-}2.5}$. The Ca and partly also Fe pattern is lacking a peak or is even slightly depleted in the core, and then decreases more strongly at the rims (Figure 4), where Ca zoning is patchy. The garnet cores are enriched in spessartine. The garnet crystals contain numerous inclusions within the whole grain volume but inclusions get less abundant towards the outer rim in most of the garnet. Inclusions comprise titanite, rutile, quartz, plagioclase, hematite, clinopyroxene, and amphibole.

Clinopyroxene can be found as inclusions in garnet and in the matrix. In both cases, it is omphacite with a jadeite component of 39%–40%. In some places, omphacite is retrogressively replaced by plagioclase and clinopyroxene, which corresponds to omphacite or diopside with varying

TABLE 1 XRF analyses of all dated eclogites

	VAI 6	TS 2	TS 1706	TS 1764
SiO_2 (%)	46.1	49.6	47.8	48.1
Al_2O_3 (%)	14.7	14.5	13.4	14.7
Fe_2O_3 (%)	15.7	12.2	14.4	11.4
MnO (%)	0.35	0.20	0.23	0.19
MgO (%)	5.86	6.71	6.83	7.97
CaO (%)	11.9	10.0	9.72	9.86
Na_2O (%)	2.87	3.65	2.59	3.39
K_2O (%)	0.04	0.43	0.35	0.50
TiO_2 (%)	1.65	1.98	1.81	1.50
P_2O_5 (%)	0.17	0.17	0.15	0.13
LOI (%)	<0.1	<0.1	1.69	0.76
Total (%)	99.59	99.51	99.98	98.82

TABLE 2 Representative electron microprobe analyses of most abundant minerals of sample VAI 6

Sample	VAI 6	VAI 6	VAI 6	VAI 6	VAI 6	VAI 6	VAI 6
Mineral	Grt	Grt	Omp	Cpx	Pl	Amp	Amp
An. Point	Core	Rim	Matrix	Sympl.		grt incl.	grt rim
SiO_2	38.8	39.3	54.1	51.7	65.7	39.4	42.4
TiO_2	0.18	0.14	0.32	0.20	bd	1.17	0.16
Al_2O_3	21.5	21.5	10.5	5.78	22.4	18.4	16.6
FeO	25.8	24.8	7.35	10.3	0.25	19.4	17.1
MnO	1.16	0.41	0.04	0.09	bd	0.03	0.05
MgO	2.81	5.03	8.13	10.4	0.01	6.32	8.69
CaO	11.5	10.8	14.6	18.1	2.6	9.28	10.89
Na_2O	0.03	bd	5.99	3.06	9.67	4.16	3.15
K_2O	bd	bd	bd	0.01	0.02	0.19	0.05
Cr_2O_3	0.01	0.03	0.02	0.04	bd	0.04	0.05
Total	101.8	102.1	101.1	99.6	100.7	98.1	99.1
Si	6.01	6.00	1.94	1.93	11.46	5.93	6.23
Ti	0.02	0.02	0.01	0.01	0.00	0.13	0.02
Al	3.93	3.88	0.44	0.25	4.61	3.26	2.88
Fe	3.34	3.17	0.22	0.32	0.04	2.44	2.11
Mn	0.15	0.05	0.00	0.00	0.00	0.00	0.01
Mg	0.65	1.15	0.44	0.58	0.00	1.42	1.90
Ca	1.91	1.77	0.56	0.72	0.49	1.50	1.71
Na	0.01	0.00	0.42	0.22	3.27	1.21	0.90
K	0.00	0.00	0.00	0.00	0.00	0.04	0.01
Cr	0.00	0.00	0.00	0.00	0.00	0.00	0.01
Total	16.01	16.04	4.03	4.03	19.87	15.93	15.77
O	24.00	24.00	6.00	6.00	32.00	23.00	23.00

Abbreviation: bd, below detection limit.

but lower jadeite content. Omphacite grains are generally very poor of inclusions, which are quartz, zircon, calcite, and rutile. Calcite porphyroblasts (up to 1 mm in diameter) can be found in the matrix and they are essentially free of inclusions. Rutile occurs as porphyroblasts as well, which are as big as garnet and calcite crystals, containing seldom ilmenite inclusions. Plagioclase occurs in symplectites with clinopyroxene in the matrix and as inclusions in garnet, in both cases of $Ab_{78\text{-}95}$ composition. In some places, amphibole and plagioclase symplectites occur with amphibole of sadangaite to pargasite composition according to the classification scheme of Hawthorne et al. (2012), which is used for all amphibole analyses of this study. Amphiboles also occur as retrograde products at the rims of garnet and rutile, where they are sadangaite and magnesio-hornblende respectively. The amphiboles included in garnet are taramite.

In eclogite sample TS 2 (Tsäkkok Nappe, N 67°06.993′/E16°55.571′), big crystals of garnet (35 vol.%), clinopyroxene (35 vol.%), white mica (5 vol.%), and minor quartz, opaque minerals and feldspar (together 5 vol.%) are surrounded by fine-grained symplectites consisting of plagioclase and clinopyroxene or amphibole, which account for 20% of the rock volume. The high-*P* mineral assemblage consists of garnet, omphacite, phengitic white mica, rutile, and clinozoisite. Representative electron microprobe analyses of the most important minerals are presented in Table 3.

Garnet in this sample is idiomorphic to hypidiomorphic and often rimmed by retrograde amphibole. Garnet is inclusion rich and contains quartz, clinozoisite, amphibole, rutile, and ilmenite, which are more abundant in the garnet core than the rims. The composition of garnet is $Alm_{48\text{-}68}Gr_{19\text{-}28}Py_{7\text{-}28}Sps_{0.4\text{-}5.8}$. They have preserved a strong growth zoning with spessartine enrichment in the core. Almandine strongly decreases and pyrope increases towards the rim, whereas grossular shows weaker zoning with elevated contents in the core (Figure 5). The growth zonation is disrupted around some cracks and inclusions which are connected by cracks.

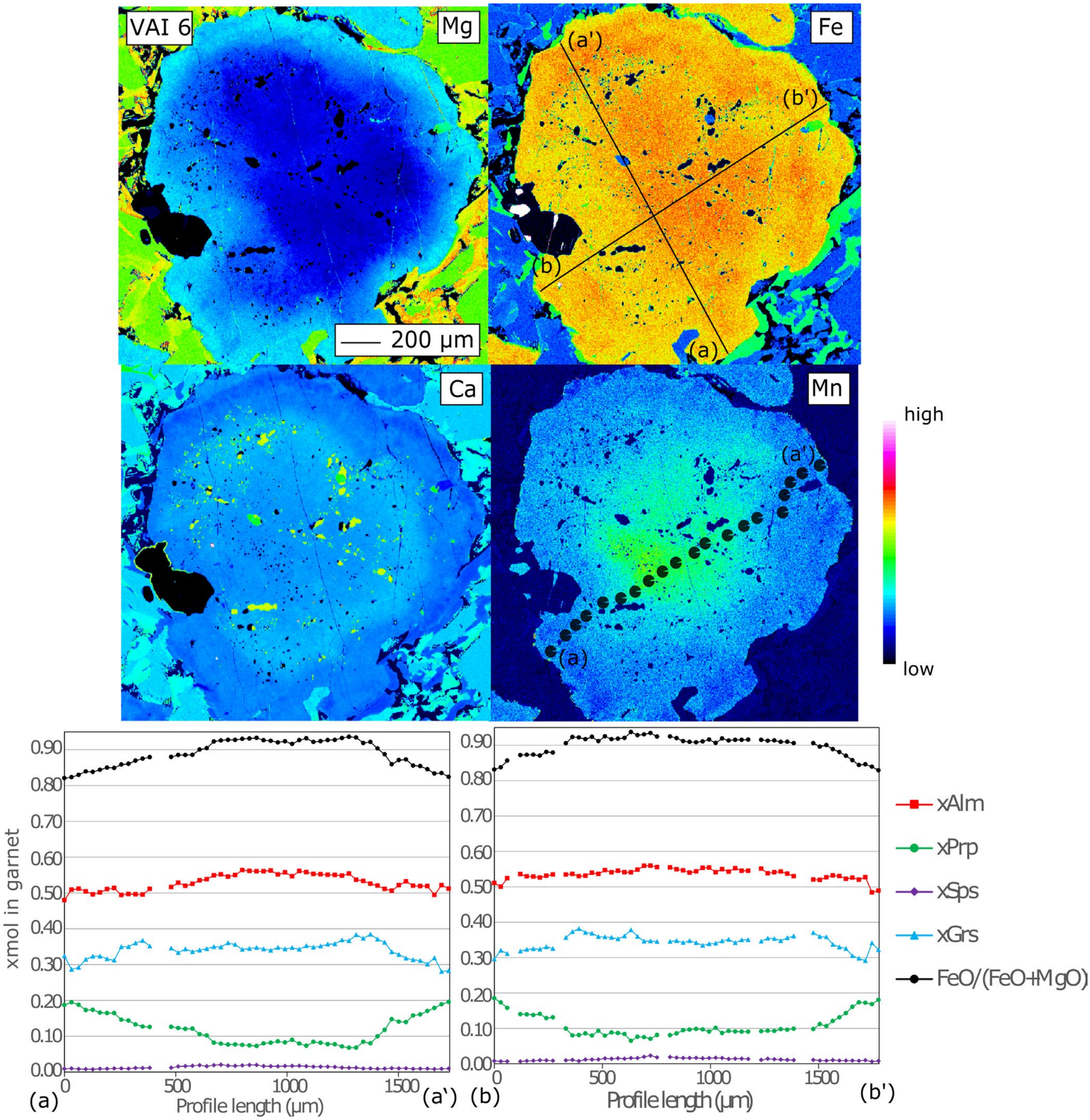

FIGURE 4 Major element distribution maps and cross sections through a representative garnet of the eclogite from Vaimok (sample VAI 6). The black lines in the Fe map mark the positions of the profiles. Black points in the Mn mark the measurement points of the LA-ICP-MS profile shown in Figure 8. Dwell time is 150 ms and map size is 620 × 610 points with 9 µm^2 pixel size. Scale of the colour bar differs between the maps

Clinopyroxene in the matrix is omphacite with $Jd_{43\text{-}45}$. Most omphacite grains are rimed by symplectites of diopside ($Jd_{3\text{-}16}$) or augite with plagioclase. The bigger omphacite grains have many inclusions of rutile, amphibole, diopside, and quartz. Phengitic white mica with up to 3.39 a.p.f.u. Si can be found in the matrix, at the rims phengite is partly overgrown by biotite. In the matrix, two compositionally different amphiboles can be found, corresponding to pargasite/sadangaite and magnesio-hornblende. Amphibole of winchite composition was found in symplectites with plagioclase, whereas pargasite/sadangaite occurs at garnet rims. Amphibole inclusions in garnet are mainly taramite but have a very variable composition. They were probably entrapped during prograde metamorphism, or they may be a retrograde phase replacing other primary inclusions. Epidote occurs in the matrix and as inclusions in garnet. Clinozoisites contain

TABLE 3 Representative electron microprobe analyses of most abundant minerals of sample TS 2

Sample	TS 2	TS 2	TS 2	TS 2	TS 2	TS 2	TS 2	TS 2	TS 2	TS 2	TS 2
Mineral	Grt	Grt	Omp	Cpx	Ph	Bt	Pl	Amp1	Amp2	Amp	Czo
An. Point	Core	Rim	Matrix	Sympl.				Matrix	Matrix	Sympl.	
SiO_2	38.6	39.2	55.9	53.1	52.5	38.7	69.1	49.2	39.2	51.1	38.6
TiO_2	0.14	0.04	0.17	0.14	0.6	1.32	0.02	0.18	0.96	0.24	0.26
Al_2O_3	21.00	22.2	10.9	3.17	28.3	17.5	20.5	8.86	19.3	6.36	27.4
FeO	27.2	23.2	4.63	6.01	1.96	15.9	0.15	12.4	12.9	9.32	8.19
MnO	0.98	0.15	bd	0.03	bd	0.04	bd	0.04	0.04	0.04	0.05
MgO	3.17	6.17	8.67	13.2	3.64	13.3	0.01	13.9	9.97	16.8	0.03
CaO	9.05	8.86	13.6	22.7	bd	0.03	0.17	10.3	11.5	12.3	23.8
Na_2O	0.10	bd	6.75	1.25	0.68	0.11	11.5	2.42	2.48	1.49	bd
K_2O	0.01	0.01	0.02	0.02	9.93	9.87	0.07	0.25	1.47	0.24	0.02
Cr_2O_3	0.02	0.03	0.12	0.06	bd	0.07	0.02	0.03	0.07	bd	0.06
Total	100.3	99.7	100.8	99.7	97.8	96.8	101.5	97.33	96.5	97.7	98.3
Si	6.07	6.03	1.98	1.96	3.39	2.84	11.89	7.12	5.80	7.28	2.92
Ti	0.02	0.00	0.00	0.00	0.03	0.07	0.00	0.02	0.11	0.03	0.01
Al	3.89	4.03	0.46	0.14	2.16	1.51	4.16	1.51	3.37	1.07	2.44
Fe	3.58	2.99	0.14	0.19	0.11	0.98	0.02	1.50	1.60	1.11	0.52
Mn	0.13	0.02	0.00	0.00	0.00	0.00	0.00	0.00	0.01	0.00	0.00
Mg	0.74	1.42	0.46	0.73	0.35	1.45	0.00	3.00	2.20	3.57	0.00
Ca	1.52	1.46	0.52	0.90	0.00	0.00	0.03	1.60	1.82	1.88	1.93
Na	0.03	0.00	0.46	0.09	0.08	0.02	3.83	0.68	0.71	0.41	0.00
K	0.00	0.00	0.00	0.00	0.82	0.92	0.01	0.05	0.28	0.04	0.00
Cr	0.00	0.00	0.00	0.00	0.00	0.00	0.00	0.00	0.01	0.00	0.00
Total	15.99	15.95	4.02	4.01	6.96	7.80	19.95	15.47	15.89	15.39	7.84
O	24.00	24.00	6.00	6.00	11.00	11.00	32.00	23.00	23.00	23.00	12.00

Abbreviation: bd, below detection limit.

6–11 wt% of iron and some of them show a considerable allanite component. There is no difference between the composition of clinozoisite in the matrix and inclusions. Plagioclase of 85–96 mol% albite component is present only in symplectites with clinopyroxene and amphibole. Rutile, ilmenite, and titanite as Ti-bearing phases sometimes occur together. Rutile is overgrown by ilmenite and titanite, indicating that rutile was the stable phase at peak metamorphic conditions, whereas ilmenite and titanite grew during exhumation.

Eclogite sample TS 1706 (Tsäkkok Nappe, N 67°07.010′/ E16°36.317′) shows a typical basaltic composition (Table 1). The peak pressure metamorphic assemblage consists of 40 vol.% garnet, 30 vol.% omphacite, 10 vol.% amphibole, 5 vol.% quartz, and 5 vol.% of other mineral phases, including phengitic white mica, rutile, and opaque minerals. Omphacite is partly replaced by symplectites of Na-poorer clinopyroxene and plagioclase, which account for 10% of the rock volume. Representative electron microprobe analyses of these minerals are shown in Table 4. Two texturally different types of garnet can be found: (a) Large garnet up to 500 μm in size and (b) clusters of small garnet that seem to merge into the bigger ones, often being aligned and forming a vein-like texture. Both garnet types preserve a prograde growth zoning with elevated Fe, Ca, and Mn in the core and elevated Mg in the rim. The garnet are more strongly zoned in Fe and Mg, than in Ca (Figure 6).

The composition of matrix garnet is $Alm_{46\text{-}67}Gr_{20\text{-}27}Py_{7\text{-}33}Sps_{0.3\text{-}2.3}$ (Figure 6), whereas that of the vein garnet is the same as the rims of the matrix garnet. The garnet grains contain inclusions of titanite, rutile, quartz, ilmenite, epidote, clinopyroxene (augite), amphibole, mica, calcite, and chlorite. Clinopyroxene in the matrix is omphacite with $Jd_{41\text{-}45}$ and some grains are rimmed by up to 10 μm wide symplectites of plagioclase and clinopyroxene with ca. 15 mol% Jd. Pargasite and magnesio-hornblende occur as inclusions in garnet, amphiboles in the matrix correspond to winchite and they are zoned with respect to Fe and Mg. Plagioclase is present in symplectites and shows Ab_{88} composition. Phengitic white mica with up to 3.43 a.p.f.u. Si occurs in the matrix and belongs to the peak metamorphic assemblage. Biotite forms inclusions in garnet.

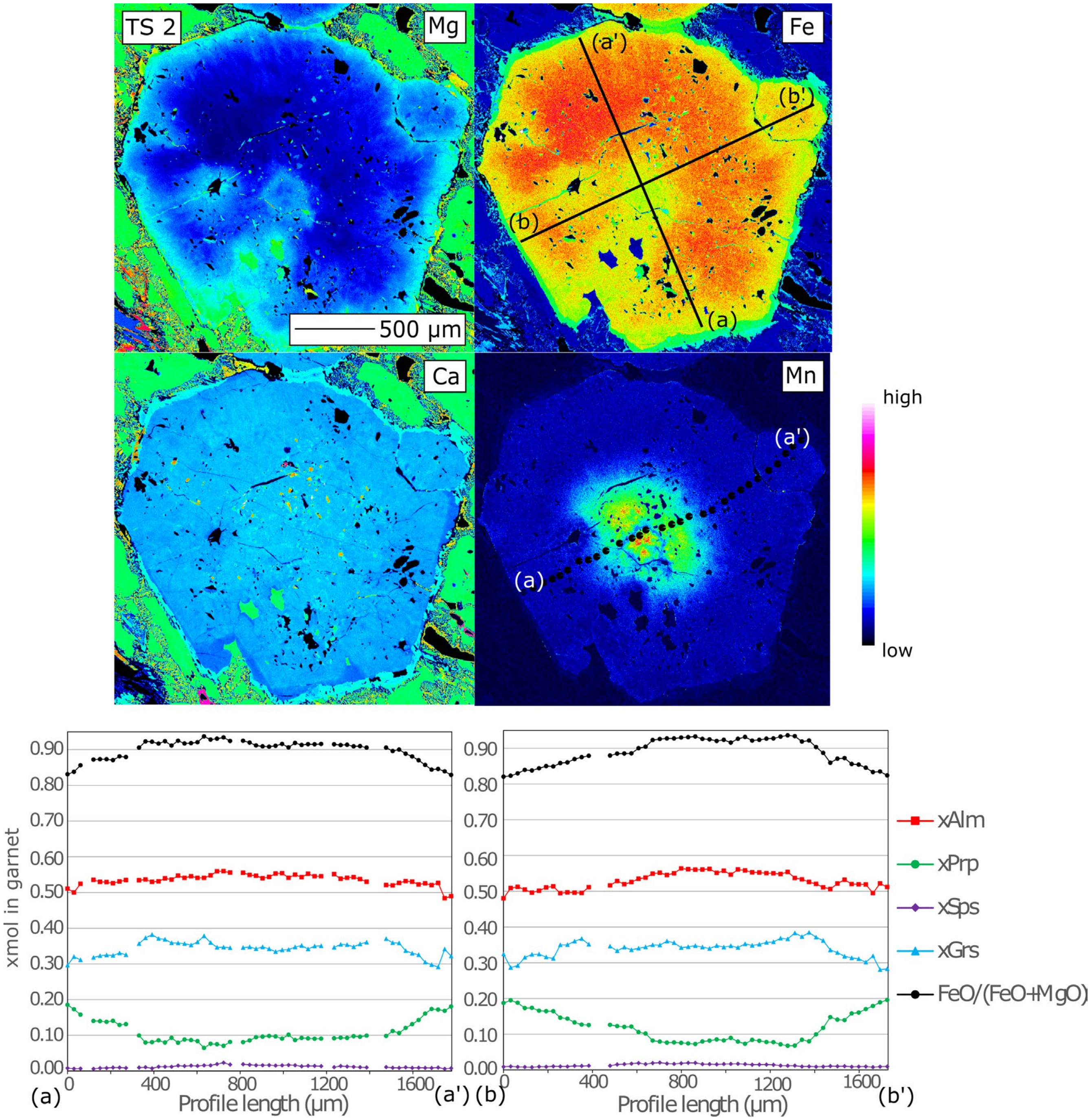

FIGURE 5 Major element distribution maps and cross-sections through a representative garnet of sample TS 2. The black lines in the Fe map mark the position of the profiles. Black points in the Mn mark the measurement points of the LA-ICP-MS profile shown in Figure 8. Dwell time is 150 ms and map size is 750 × 750 points with 9 μm^2 pixel size. Scale of the colour bar differs between maps

The typical basaltic eclogite sample TS 1764 (Table 1, Tsäkkok Nappe, N 67°6.994′/E16°57.311′) shows large garnet porphyroblasts in a matrix consisting mostly of symplectites, but also well-preserved grains of omphacite, epidote, mica, rutile, amphibole, and opaque minerals. The high-*P* mineral assemblage consists of garnet, omphacite, phengitic white mica, rutile, and amphibole. Mineral chemistry of the most abundant minerals is shown in Table 5.

Garnet is 1–2 mm in diameter and rich in inclusions of amphibole, rutile, quartz, Fe-ore, and epidote. There are up to 50 µm wide veins (comprising matrix minerals) that run through the garnet grains. Garnet is mostly rimed by amphibole. Despite such a retrograde replacement, garnet grains still preserve their original growth zoning with clearly elevated Fe and Mn composition in the core, clearly elevated Mg composition at the rim and almost no zoning in

TABLE 4 Representative electron microprobe analyses of most abundant minerals of sample TS 1706

Sample	TS 1706	TS 1706	TS 1706	TS 1706	TS 1706	TS 1706	TS 1706	TS 1706	TS 1706
Mineral	Grt	Grt	Omp	Cpx	Cpx	Pl	Amp1	Amp2	Ph
An. Point	Core	Rim		sympl.	grt incl.		Matrix	grt incl.	
SiO_2	37.5	38.2	55.9	54.9	54.1	66.2	52.9	41.8	52.0
TiO_2	0.25	bd	0.12	0.29	0.20	bd	0.16	0.15	0.43
Al_2O_3	21.2	21.9	9.97	4.42	11.4	19.9	9.28	14.2	27.3
FeO	28.1	24.4	4.18	5.13	12.1	0.33	7.71	18.9	2.15
MnO	1.13	0.14	0.03	0.04	0.03	0.04	0.03	0.03	0.05
MgO	2.57	6.01	9.15	13.2	10.1	0.63	16.1	7.77	3.52
CaO	8.65	8.43	14.3	19.8	10.3	2.30	8.14	10.6	0.01
Na_2O	0.11	0.03	6.01	1.31	1.92	9.79	3.68	2.82	0.52
K_2O	bd	0.02	bd	0.03	0.47	0.03	0.22	0.02	9.65
Cr_2O_3	bd	bd	0.01	0.05	0.23	0.10	bd	bd	0.02
Total	99.5	99.01	99.6	99.1	100.7	99.3	98.2	96.3	95.6
Si	5.98	5.97	2.00	2.00	1.94	11.71	7.36	6.39	3.43
Ti	0.03	0.00	0.00	0.01	0.01	0.00	0.02	0.02	0.02
Al	3.98	4.03	0.42	0.19	0.48	4.15	1.52	2.56	2.13
Fe	3.75	3.19	0.12	0.16	0.36	0.05	0.90	2.42	0.12
Mn	0.15	0.02	0.00	0.00	0.00	0.01	0.00	0.00	0.00
Mg	0.61	1.4	0.49	0.72	0.54	0.17	3.34	1.77	0.35
Ca	1.48	1.41	0.55	0.77	0.39	0.44	1.21	1.73	0.00
Na	0.03	0.01	0.42	0.09	0.13	3.36	0.99	0.84	0.07
K	0.00	0.00	0.00	0.00	0.02	0.01	0.04	0.00	0.81
Cr	0.00	0.00	0.00	0.00	0.01	0.01	0.00	0.00	0.00
Total	16.01	16.03	4.00	3.94	3.89	19.89	15.38	15.73	6.92
O	24.00	24.00	6.00	6.00	6.00	32.00	23.00	23.00	11.00

Abbreviation: bd, below detection limit.

Ca (Figure 7). The overall composition of garnet is $Alm_{46-68}Gr_{19-25}Py_{8-29}Sps_{0.4-6.7}$. Omphacite ($Jd_{39-44}$) in the matrix is partly replaced by the symplectites consisting of plagioclase, diopsidic clinopyroxene, and amphibole. Phengitic white mica, often surrounded by biotite, occurs in the matrix and in the veins within the garnet. Phengite, with 3.40 Si a.p.f.u. is part of the peak metamorphic assemblage, whereas biotite is a retrograde phase. Amphibole can be found in the matrix and around garnet. Matrix amphibole is winchite and we consider it as belonging to the peak metamorphic assemblage, whereas amphibole around garnet is sadangaite of retrograde origin.

4.2 | Pressure–temperature estimates

According to a recent publication, Vaimok eclogites reached UHP metamorphic conditions of 28–31 kbar at 660–780°C (for more details see Bukała et al., 2018). Here we provide the *P–T* constraints for Tsäkkok eclogites only. Peak metamorphic conditions of the investigated Tsäkkok eclogites have been calculated on the basis of the mineral assemblage garnet+omphacite+phengite. The compositions of garnet rims, omphacite and phengite as shown in Tables 3–5 were selected for calculations. We used a combination of (a) the garnet–clinopyroxene Fe–Mg exchange thermometer (Ravna, 2000) and (b) the net-transfer reaction 6 diopside + 3 muscovite = 3 celadonite + 2 grossular + pyrope calibrated by Ravna and Terry (2004). Calculations were performed with the thermodynamic data of Holland and Powell (1998) and the activity models for the phengite solid solution (Holland & Powell, 1998), clinopyroxene (Holland, 1990), and garnet (Ganguly et al., 1996), as recommended by Ravna and Terry (2004). The results yield a maximum pressure of ~25 kbar at 590°C (sample TS 2), ~26 kbar at 650°C (sample TS 1706) and ~25 kbar at 664°C (sample TS 1764) obtained from intersections between the reactions

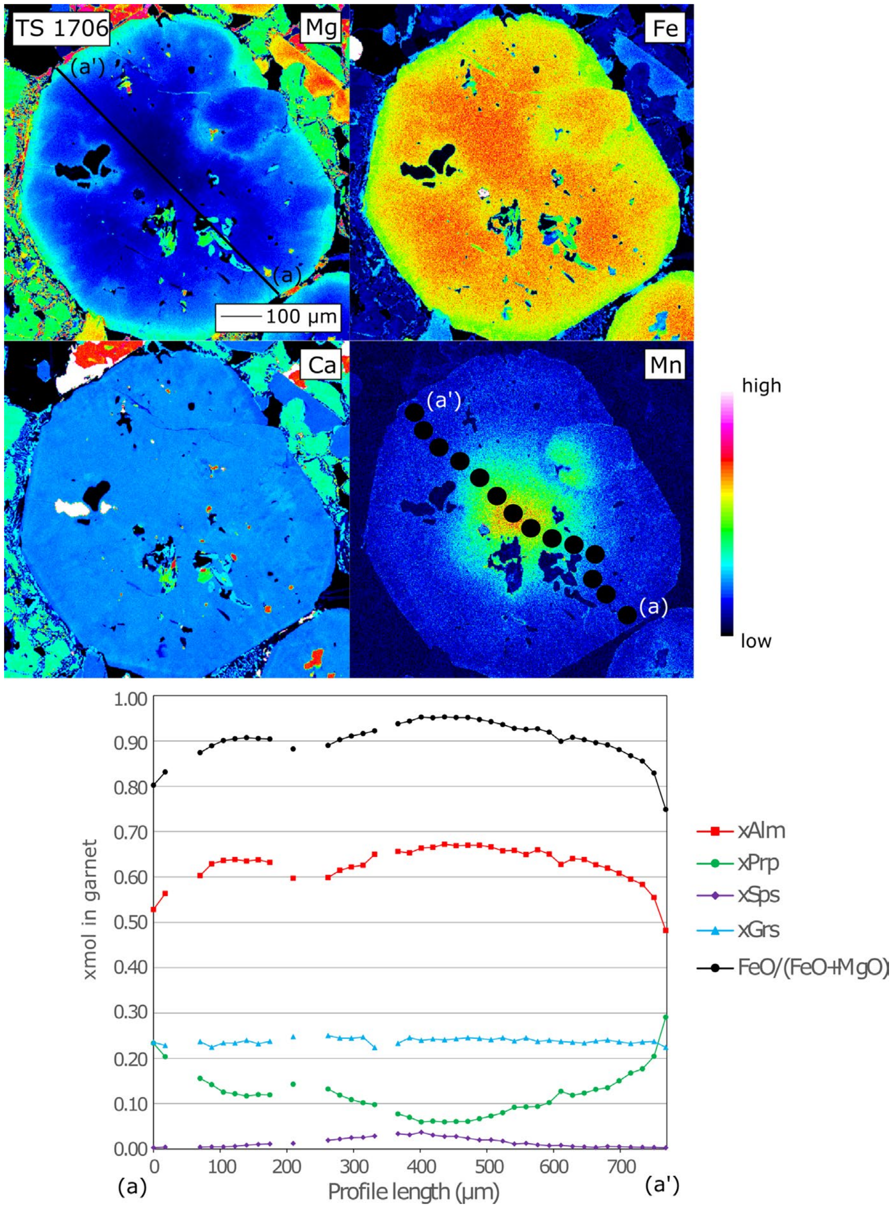

FIGURE 6 Major element distribution maps and cross-sections through a representative garnet of sample TS 1706. The black line in the Mg map marks the position of the profile. Black points in the Mn mark the measurement points of the LA-ICP-MS profile shown in Figure 8. Dwell time is 100 ms and map size is 550 × 550 points with 2.25 μm^2 pixel size. Scale of the colour bar differs between maps

(1) and (2). Uncertainty related to the oxidation state of iron can be the main problem concerning the calculated temperature.

4.3 | Laser Analyses

In sample VAI 6, garnet preserved its growth zoning as it is anticipated from the major element profiles and maps (Figure 4), as well as the Lu profiles through the garnet (Figure 8). The Lu profile in sample VAI 6 does not show a simple bell-shaped pattern, but rather a high peak in the core with slightly lower peaks, that is, two intersections with a spherical maximum, near the garnet rims.

In the profile through a garnet grain from sample TS 2, Lu is strongly enriched in the core (17 ppm) compared to the rims (<1 ppm). As it was already inferred from the major-element distribution (Figure 5), this garnet retained its original growth zoning, which is reflected by the Lu abundance. In addition to the strong enrichment in the garnet core, there are also smaller peaks near the rims, which are similar to sample VAI 6, although less pronounced.

In sample TS 1706 a small spot size (44 μm) for the Lu analysis in the garnet was chosen and only 14 points were measured since garnet in this sample are small (Figure 6). Therefore, the Lu peaks are not very distinct but growth zoning with a central peak and two smaller peaks towards the rims can be observed.

In the garnet profile of sample TS 1764 Lu is extremely enriched in the core with up to 90 ppm, whereas rim concentration is below 1 ppm. All four eclogite samples thus show well-preserved garnet growth zoning by their Lu distribution.

TABLE 5 Representative electron microprobe analyses of most abundant minerals of sample TS 1764

Sample	TS 1764	TS 1764	TS 1764	TS 1764	TS 1764	TS 1764	TS 1764	TS 1764
Mineral	Grt	Grt	Omp	Ep	Ph	Bt	Amp	Amp
An. Point	Core	Rim					matrix	grt rim
SiO_2	37.6	38.8	56.1	38.6	52.0	36.1	51.9	39.5
TiO_2	0.18	0.11	0.08	bd	0.46	0.06	0.05	0.04
Al_2O_3	21.2	22.3	10.6	24.3	29.5	19.9	9.22	17.1
FeO	29.1	22.7	3.29	12.0	1.46	16.0	9.75	16.2
MnO	1.39	0.23	0.01	0.13	0.01	0.04	0.08	0.11
MgO	2.12	7.75	9.18	0.02	3.23	13.8	14.6	9.33
CaO	8.75	8.74	14.1	23.8	bd	bd	8.28	11.3
Na_2O	0.09	0.15	6.13	bd	1.10	0.18	3.12	2.61
K_2O	bd	0.01	bd	0.04	9.60	10.3	0.21	1.14
Cr_2O_3	bd	0.01	0.26	0.01	0.05	bd	bd	bd
Total	100.5	100.7	99.8	98.9	97.5	96.3	97.2	97.3
Si	5.97	5.91	1.99	2.97	3.36	2.68	7.36	5.97
Ti	0.02	0.01	0.00	0.00	0.02	0.00	0.01	0.00
Al	3.97	4.01	0.44	2.21	2.25	1.74	1.54	3.05
Fe	3.87	2.89	0.10	0.77	0.08	0.99	1.16	2.05
Mn	0.19	0.03	0.00	0.01	0.00	0.00	0.01	0.01
Mg	0.50	1.76	0.49	0.00	0.31	1.52	3.09	2.10
Ca	1.49	1.43	0.54	1.96	0.00	0.00	1.26	1.83
Na	0.03	0.04	0.42	0.00	0.14	0.03	0.86	0.76
K	0.00	0.00	0.00	0.00	0.79	0.98	0.04	0.22
Cr	0.00	0.00	0.01	0.00	0.00	0.00	0.00	0.00
Total	16.03	16.09	3.99	7.93	6.95	7.95	15.31	15.99
O	24.00	24.00	6.00	12.00	11.00	11.00	23.00	23.00

Abbreviation: bd, below detection limit.

4.4 | Lu–Hf geochronology

For sample VAI 6 four garnet separates, one tabletop-digested whole-rock split and one bomb-digested whole-rock split were analysed. All six separates yield an age of 480.4 ± 1.2 Ma (MSWD = 0.61, n = 6, Figure 9). Absolute Hf content varies between 0.102 and 0.122 ppm for the garnet separates, 0.748 ppm for the tabletop whole rock, and 3.00 ppm for the bombed whole rock. The complete Lu–Hf data can be found in Table 6. The higher Hf content in the bombed whole rock when compared to the tabletop-digested whole rock shows that Hf-rich phases are present which are only digested under pressure (e.g. zircon, rutile). However, these phases cannot be significantly older than the eclogite assemblage, as both whole-rock splits fit perfectly on the same isochron with the garnet.

Four garnet separates, one clinopyroxene separate, and two whole-rock splits were analysed for sample TS 2. One of the whole-rock splits was digested in a Parr bomb, also digesting Hf-rich minerals like zircon and rutile, and one was digested with the tabletop procedure, leaving those phases behind. Absolute Hf contents in mineral separates are 0.306–0.363 ppm, for the tabletop-digested whole-rock 0.490 ppm, and for the bomb-digested whole-rock 3.11 ppm. $^{176}Lu/^{177}Hf$ ratios in garnet separates are extraordinarily small with 0.4355–0.5224, while the ratios for the clinopyroxene separate, the bombed whole rock and the tabletop-digested whole rock are 0.003504, 0.02353, and 0.1461. All isotope data are shown in Table 6. An isochron is shown in Figure 9 and gives an age of 487.7 ± 4.6 Ma (MSWD = 0.44, n = 7).

For sample TS 1706 one clinopyroxene separate, four garnet separates and three whole-rock splits (one bomb- and two tabletop digested) were analysed. Absolute Hf contents and isotope ratios are similar to those of sample TS 2 and are shown in Table 6. All of the measured separates yield an age of 484.6 ± 4.6 Ma (MSWD = 1.9, n = 8, Figure 9). Four garnet separates, one clinopyroxene separate, one bomb-digested whole-rock split and one tabletop-digested whole-rock split

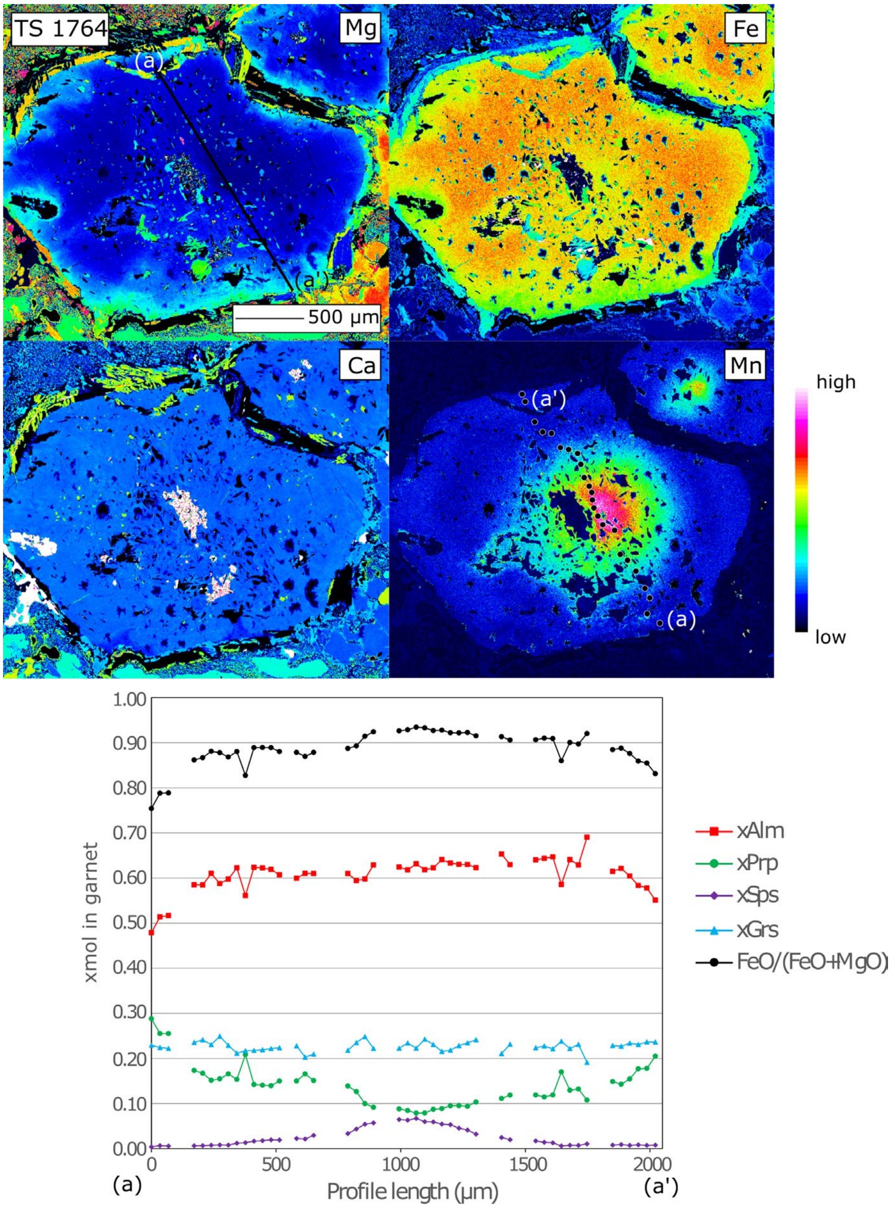

FIGURE 7 Major element distribution maps and cross section through a representative garnet of sample TS 1764. The black line in the Mg map marks the position of the profile. Black points in the Mn mark the measurement points of the LA-ICP-MS profile shown in Figure 8. Dwell time is 100 ms and map size is 800 × 700 points with 12.25 µm^2 pixel size. Scale of the colour bar differs between maps

were measured from sample TS 1764. This sample is quite similar to the other samples from the Tsäkkok Lens with respect to Lu and Hf isotopic compositions. Figure 9 shows the isochron giving an age of 486.2 ± 3.2 Ma (MSWD = 0.54, $n = 7$).

5 | DISCUSSION

5.1 | Dating of Vaimok eclogite

Garnet of eclogite VAI 6 mostly retained growth zoning in major element contents. The Lu profile (Figure 8) shows enrichment in the garnet core (~3.5 ppm), and smaller peaks towards the garnet rims (~2 ppm). According to Skora et al. (2006), such zoning reflects an increase in the diffusion rate at higher temperatures near the peak temperature of metamorphism which allows Lu to reach the garnet from more distant parts of the matrix. The Lu distribution thus clearly reflects growth of garnet and the Lu–Hf age dates prograde metamorphism. A statistically well-defined isochron (MSWD = 0.61) yields an age of 480.4 ± 1.2 Ma (Figure 9). This supports the ages obtained by U–Pb geochronology on zircon (481.9 ± 1.0 Ma; Root & Corfu, 2012) and it is younger than the Sm–Nd age of 503 ± 14 Ma obtained by Mørk et al. (1988; Figure 10). Root and Corfu (2012) already proposed that the older age obtained by Sm–Nd is probably due to isotopic disequilibrium or caused by inherited inclusions. Our results support this. The temperature conditions during metamorphism are distinctly higher in the Vaimok Lens (~28–31 kbar and 660–780°C; Bukała et al., 2018), when compared to the Tsäkkok Lens (~25–26 kbar and 590–660°C; Figure 11). Nevertheless, also the higher temperature recorded in the Vaimok Lens is below the closure temperature

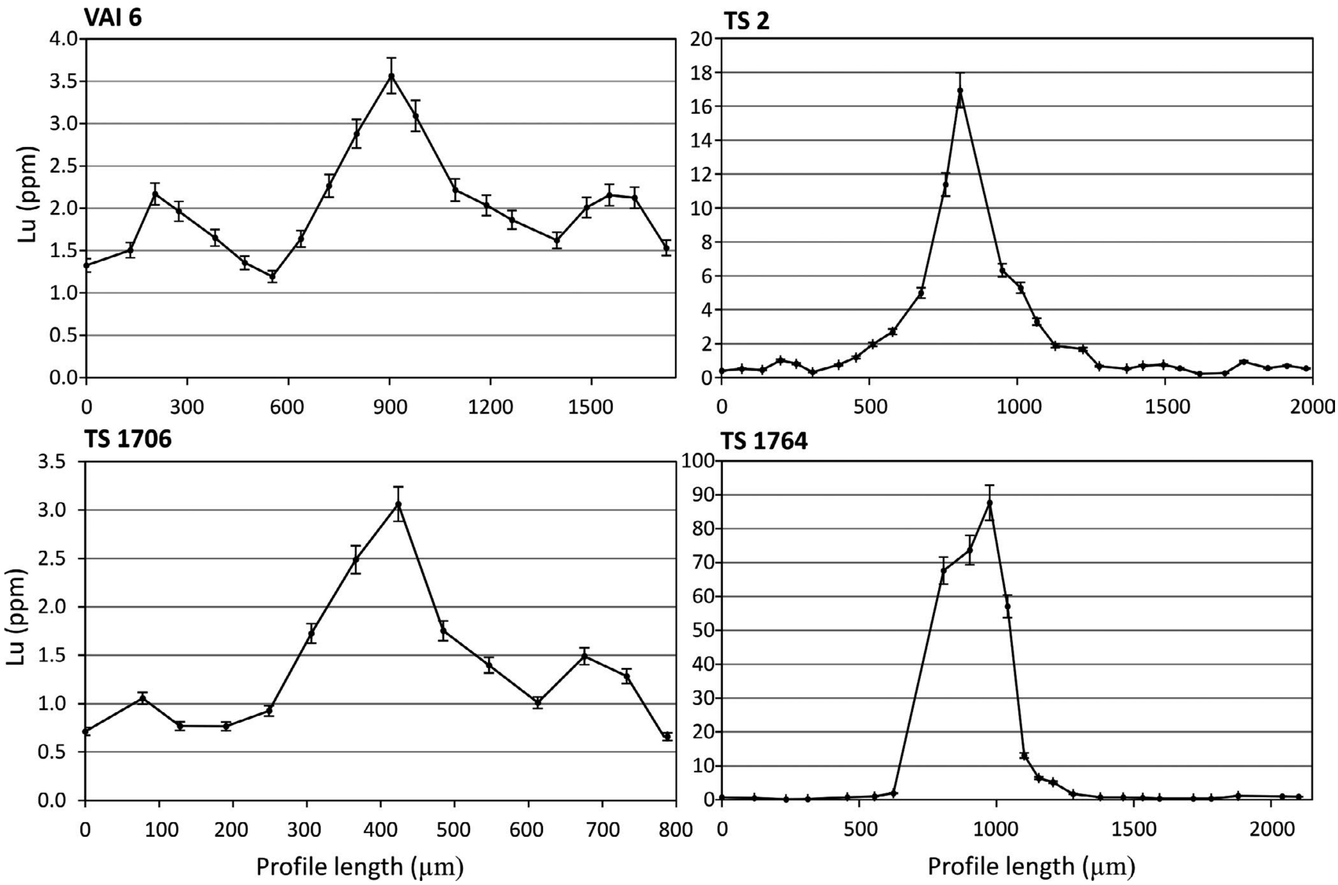

FIGURE 8 Lu abundance profiles through the garnet grains. Distribution of measured points is shown in the major element maps (Figures 4–7), all profiles run from (a) (left) to (a′) (right). The Lu profiles were obtained with LA-ICP-MS

of the Lu–Hf system in garnet, which is estimated to be above 900°C (Scherer et al., 2000; Smit et al., 2013). The idea that the sample from the Vaimok Lens never exceeded the closure temperature is supported by the fact that Lu distribution does not show an increase in Lu towards the outer rim of the garnet and growth zoning is preserved.

The most precise ages obtained by U–Pb on zircon and Lu–Hf on garnet overlap within error and therefore we interpret *c*. 480 Ma as dating the age of prograde to peak metamorphism. A recent U–Th-total-Pb monazite age of 498 ± 10 Ma, which was interpreted to date prograde metamorphism in the presence of garnet (Barnes et al., 2018), is slightly older than our results. This age may be related to a very early phase of subduction, while our age is nearer to peak pressure conditions. However, it is also possible that a significant amount of common Pb was incorporated in those monazites, which is not distinguished in this method. This should be tested by isotope analysis before further interpretation.

5.2 | Dating of Tsäkkok eclogites

Eclogites from the Tsäkkok Lens preserved their peak metamorphic mineral assemblage with only minor signs of retrogression and as shown above, garnet shows prograde growth distribution of major elements and Lu. The laser ablation profile of garnet from sample TS 1764 shows strong enrichment of Lu in the core (90 ppm). Therefore, we interpret the age of this sample as dating prograde garnet growth. The other two samples from the Tsäkkok Nappe show a similar Lu distribution as sample VAI 6 from the Vaimok Nappe. While the difference in Lu between the core and rim peaks of sample TS 1706 is similar to sample VAI 6, the rim peaks in sample TS 2 are less pronounced, or the core peak is higher (2–3 ppm in sample TS 1706 vs 20–35 ppm in sample TS 2). Sample TS 1706 has, by far, the lowest Lu content in the garnet core (as measured by LA-ICP-MS). However, Lu contents in garnet separates measured with the MC-ICPMS are similar for all samples from the Tsäkkok Nappe. Therefore, the low-Lu contents in garnet from sample TS 1706 may reflect that the investigated garnet grains were not cut exactly through the centre but slightly more tangentially. To summarize, garnet in all Tsäkkok samples preserves growth zoning, Lu–Hf geochronology dates prograde garnet growth, and the ages are 487.7 ± 4.6, 486.2 ± 3.2, and 484.6 ± 4.6 Ma. These ages overlap with each other and those obtained by U–Pb geochronology on zircon (481.9 ± 1.2 Ma; Root & Corfu, 2012). Both Lu–Hf and

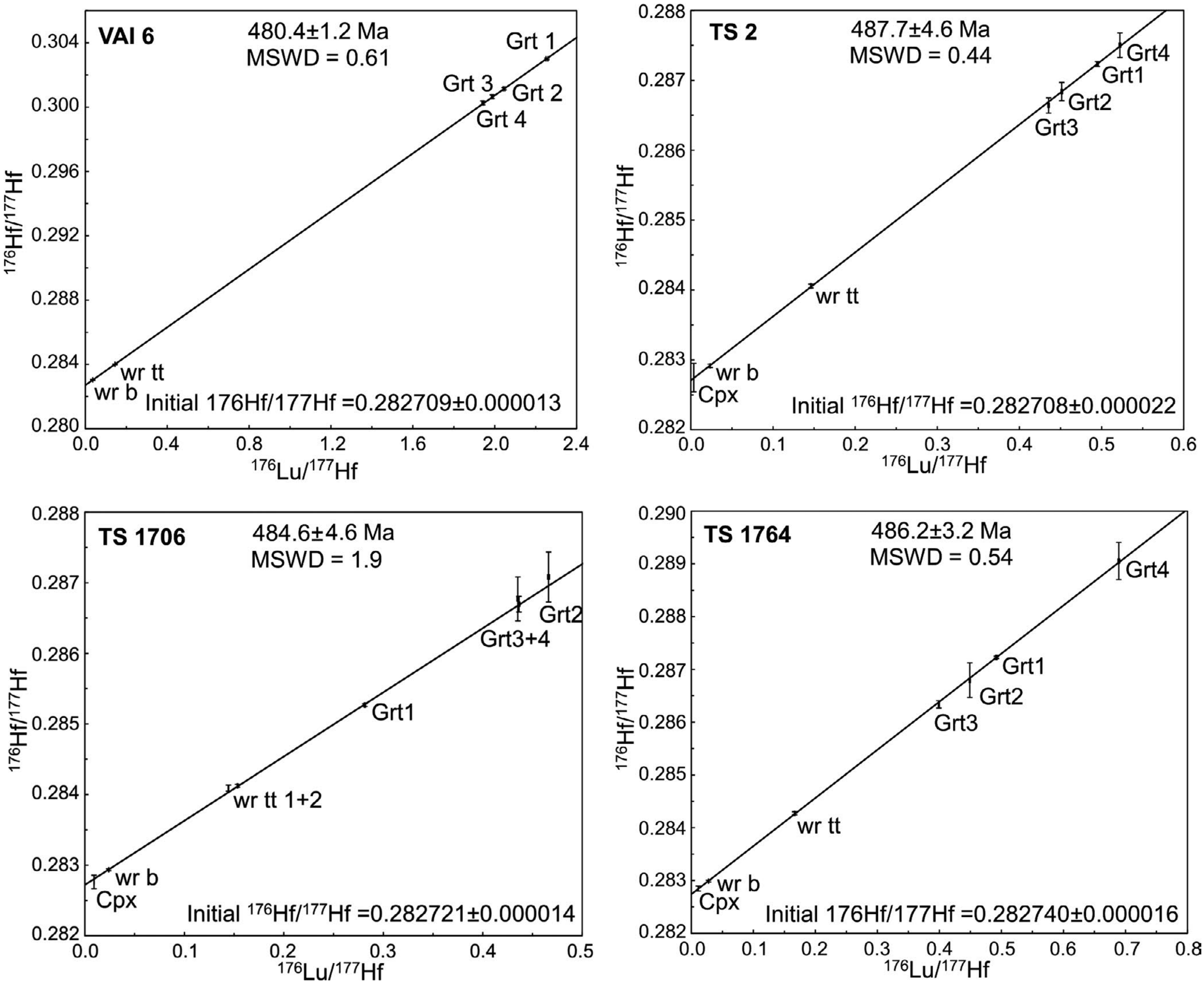

FIGURE 9 Lu–Hf isochrons for all samples, 2σ uncertainties are used. Calculated initial values and ages are based on $\lambda^{176}Lu = 1.865 \times 10$–11 yr^{-1} (Scherer et al. 2001). Grt: garnet separates, Cpx: clinopyroxene separates, wr tt: tabletop-digested whole-rock splits, wr b: bomb-digested whole-rock split

U–Pb methods provide younger ages than results from the Sm–Nd geochronology (503 ± 18 Ma; Mørk et al., 1988). The HP ages are supported by recently published in-situ white mica $^{40}Ar/^{39}Ar$ cooling ages obtained for the metasedimentary host rocks of the eclogites (*c*. 475–477 Ma; Barnes et al., 2020).

Comparing the ages from the Tsäkkok and Vaimok Lenses it seems as if the ages from the Tsäkkok Lens are slightly older. Before making this interpretation, it has to be considered that the zoning of Lu in garnet has an impact on the age and could possibly bias it. In both the sample from the Vaimok Lens and also the youngest sample from the Tsäkkok Lens (TS 1706), there are relatively high secondary Lu peaks in the garnet rim, which could bias the ages towards the rims. In the older two samples from Tsäkkok, in contrast, the secondary rims are way less pronounced, and therefore, the age could be biased more towards the core. In order to make the interpretation that the age of subduction really is slightly older in Tsäkkok when compared to Vaimok, we have to exclude the possibility that this age difference is produced by different Lu zoning in garnet. As stated above, we interpret the higher secondary peaks in sample TS 1706 as being an effect of cutting the measured sample not directly through the garnet core. This also means that the age of this sample is not biased towards the rim. For the sample from the Vaimok Lens, we cannot exclude that the age is only younger because the age is biased more towards the rim. Further analyses of more garnet from the Vaimok Lens would be necessary to resolve this. Therefore, based on the obtained data set, we conclude that the age of eclogites from the Tsäkkok Nappe is slightly older than that of eclogites from the Vaimok Nappe.

TABLE 6 Lu and Hf isotopic composition of mineral separates and whole rocks of all samples

Sample	Mineral	Lu (ppm)	Hf (ppm)	$^{176}Lu/^{177}Hf$	Error	$^{176}Hf/^{177}Hf$	Error
VAI 6	wr tt	0.761	0.748	0.1445	0.0003	0.284002	0.000024
VAI 6	wr b	0.764	3.00	0.03611	0.00007	0.283038	0.000015
VAI 6	Grt 1	1.62	0.102	2.255	0.005	0.303001	0.000056
VAI 6	Grt 2	1.62	0.113	2.046	0.004	0.301144	0.000070
VAI 6	Grt 3	1.63	0.117	1.988	0.004	0.300651	0.000117
VAI 6	Grt 4	1.66	0.122	1.941	0.004	0.300260	0.000123
TS 2	wr tt	0.504	0.490	0.1461	0.0003	0.284057	0.000027
TS 2	wr b	0.515	3.11	0.02353	0.00005	0.282916	0.000025
TS 2	Cpx	0.00896	0.363	0.003504	0.000007	0.282747	0.000203
TS 2	Grt 1	1.15	0.331	0.4949	0.0010	0.287234	0.000036
TS 2	Grt 2	1.15	0.363	0.4515	0.0009	0.286839	0.000130
TS 2	Grt 3	1.11	0.361	0.4355	0.0009	0.286641	0.000109
TS 2	Grt 4	1.13	0.306	0.5224	0.0010	0.287503	0.000176
TS 1706	wr tt 1	0.457	0.450	0.1444	0.0003	0.284092	0.000044
TS 1706	wr tt 2	0.488	0.452	0.1534	0.0003	0.284123	0.000021
TS 1706	wr b	0.492	2.91	0.02400	0.00005	0.282935	0.000014
TS 1706	Cpx	0.0167	0.256	0.009241	0.000019	0.282762	0.000095
TS 1706	Grt 1	1.24	0.627	0.2815	0.0006	0.285267	0.000019
TS 1706	Grt 2	1.26	0.384	0.4662	0.0009	0.287081	0.000353
TS 1706	Grt 3	1.25	0.407	0.4364	0.0009	0.286696	0.000112
TS 1706	Grt4	1.27	0.414	0.4353	0.0009	0.286771	0.000312
TS 1764	wr tt	0.414	0.353	0.1666	0.0003	0.284273	0.000030
TS 1764	wr b	0.455	2.34	0.02766	0.00006	0.282989	0.000018
TS 1764	Cpx	0.0209	0.264	0.01123	0.00002	0.282848	0.000047
TS 1764	Grt 1	1.54	0.446	0.4919	0.0010	0.287227	0.000023
TS 1764	Grt 2	1.53	0.484	0.4491	0.0009	0.286795	0.000327
TS 1764	Grt 3	1.49	0.531	0.3991	0.0008	0.286336	0.000069
TS 1764	Grt 4	1.77	0.365	0.6893	0.0014	0.289053	0.000352

Note: Errors on isotopic ratios are 2 *SD*.

5.3 | Regional geological context

The bulk rock analyses of the studied Vaimok and Tsäkkok samples are very similar (despite some minor differences in Si, Ca, and K content, Table 1). Nevertheless, protoliths have different origins: The protoliths of the eclogites from Vaimok are dolerite dyke swarms that intruded into a continental sedimentary series during the rifting that later opened the Iapetus Ocean at *c.* 590–610 Ma (Albrecht, 2000; Barnes et al., 2018; Root & Corfu, 2012; Svenningsen, 2001; van Roermund, 1985) and the eclogites from Tsäkkok represent former MORB with occasionally occurring pillow basalts (e.g. Kullerud et al., 1990). Therefore, we interpret the Tsäkkok Nappe as the very outer part of the ocean–continent transition zone, while the origin of the Vaimok Nappe is the continental margin. This is also reflected in the small age difference between both nappes with the more outboard Tsäkokk Lens being subducted first and later underplated by the more easterly derived (in present-day coordinates) Vaimok Lens. This fits the general structure of the Caledonian nappe stack. Metamorphic conditions of eclogites are lower in the Tsäkkok Lens (~25–26 kbar and 590–660°C) compared to the Vaimok Lens (~28–31 kbar and 660–780°C; Figure 11; Bukała et al., 2018) reflecting a difference in depth of subduction, which was already proposed by Mørk et al. (1988).

For further interpretation of the tectonic evolution, the stacking order of tectonic units is of great importance. The traditional stacking order bears more problems than the new one by Andréasson (2020). If the traditional stacking order is correct (Vaimok at the base, Sarek in the middle, Tsäkkok at the top), all these units may represent Baltica, and the uppermost (Tsäkkok) was originally closest to the ocean, which fits lithological characteristics. The slightly older age of eclogite in Tsäkkok as compared to Vaimok would also fit such a

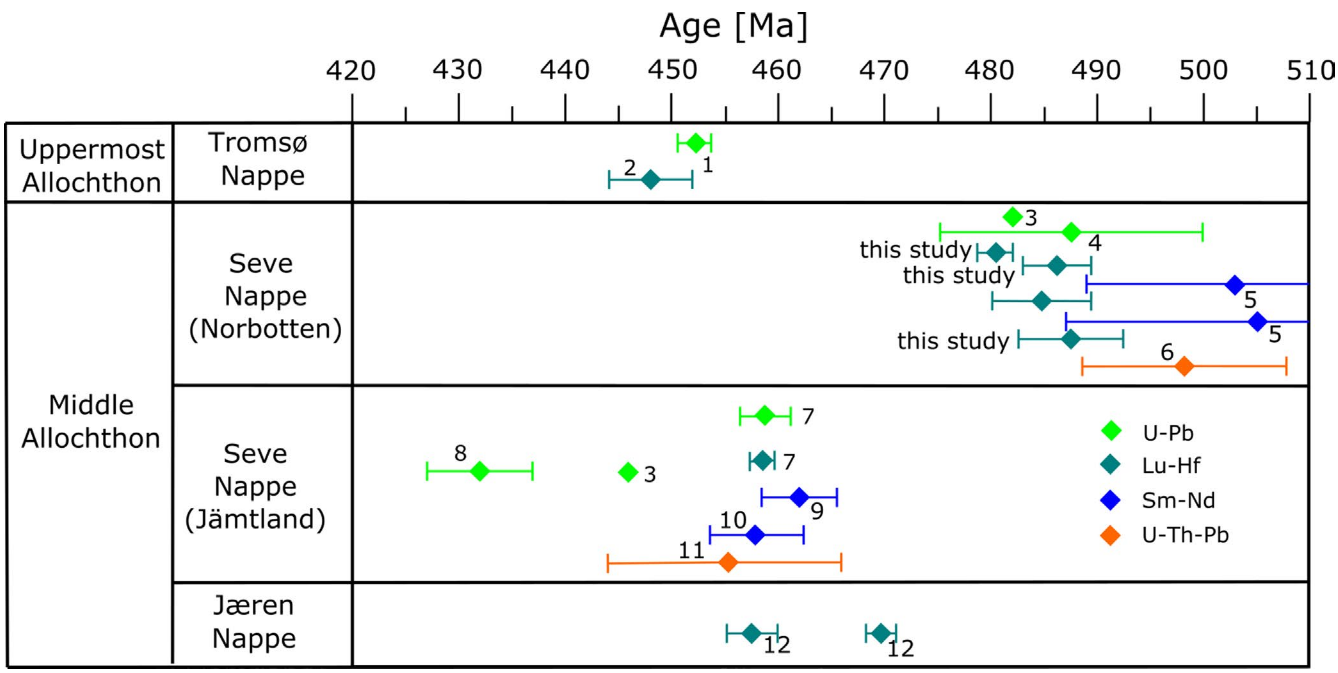

FIGURE 10 Subduction-related ages from the Scandinavian Caledonides which are older than the main Scandian collision. They are sorted by method and tectonic affiliation. 1—Corfu et al. (2003); 2—Fassmer et al. (2020); 3—Root and Corfu (2012); 4—Essex et al. (1997); 5—Mørk et al. (1988); 6—Barnes et al. (2018); 7—Fassmer et al. (2017); 8—Gromet et al. (1996); 9—Grimmer et al. (2015); 10—Brueckner and Van Roermund (2007); 11—Majka et al. (2012); 12—Smit et al. (2010)

FIGURE 11 *PT* diagram showing peak metamorphic conditions for different locations in Norrbotten and Jämtland: Tsäkkok eclogite (this study), Vaimok eclogite (Bukała et al., 2018), Friningen eclogite (Janák, van Roermund, et al., 2013), Tjeliken eclogite (Majka et al., 2014), Tjeliken micaschist (Fassmer et al., 2017), Stor Jougdan eclogite and garnet peridotite (Klonowska et al., 2016) and Åreskutan paragneiss (Klonowska et al., 2017)

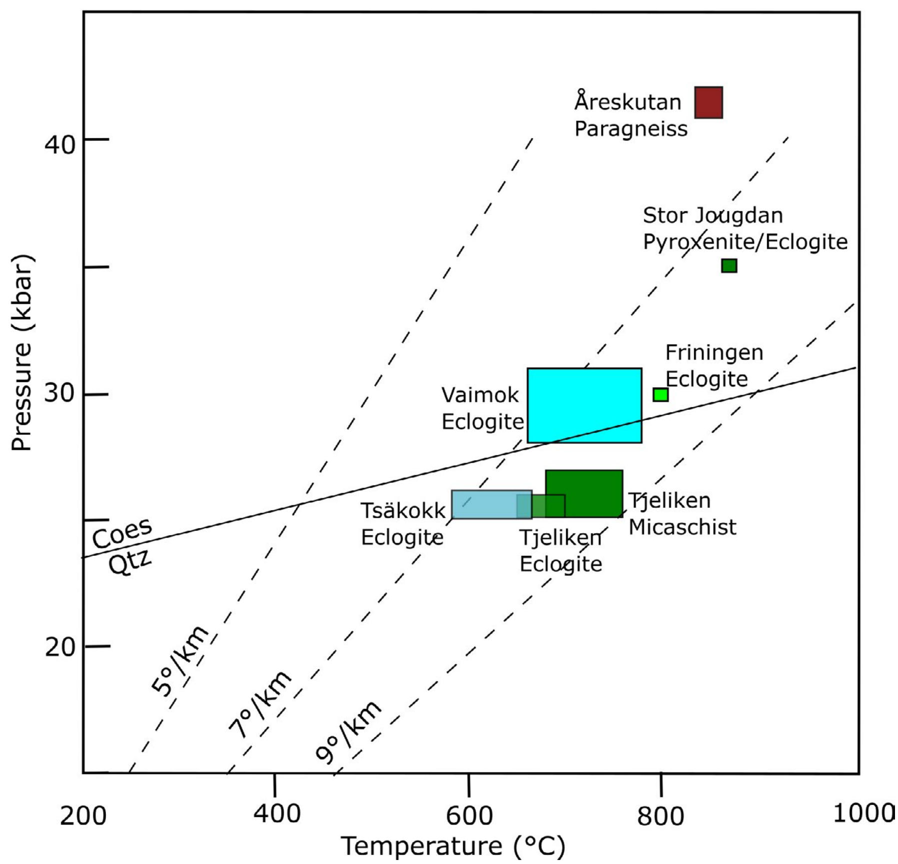

scenario because the ocean–continent transition would have been subducted first during an arc–continent collision. On the other hand, the occurrence of the medium-pressure Sarek Lens sandwiched between two high-*P* units (Vaimok and Tsäkkok) would be difficult to explain. Another problem is the age difference of eclogite between Norrbotten and Jämtland. This

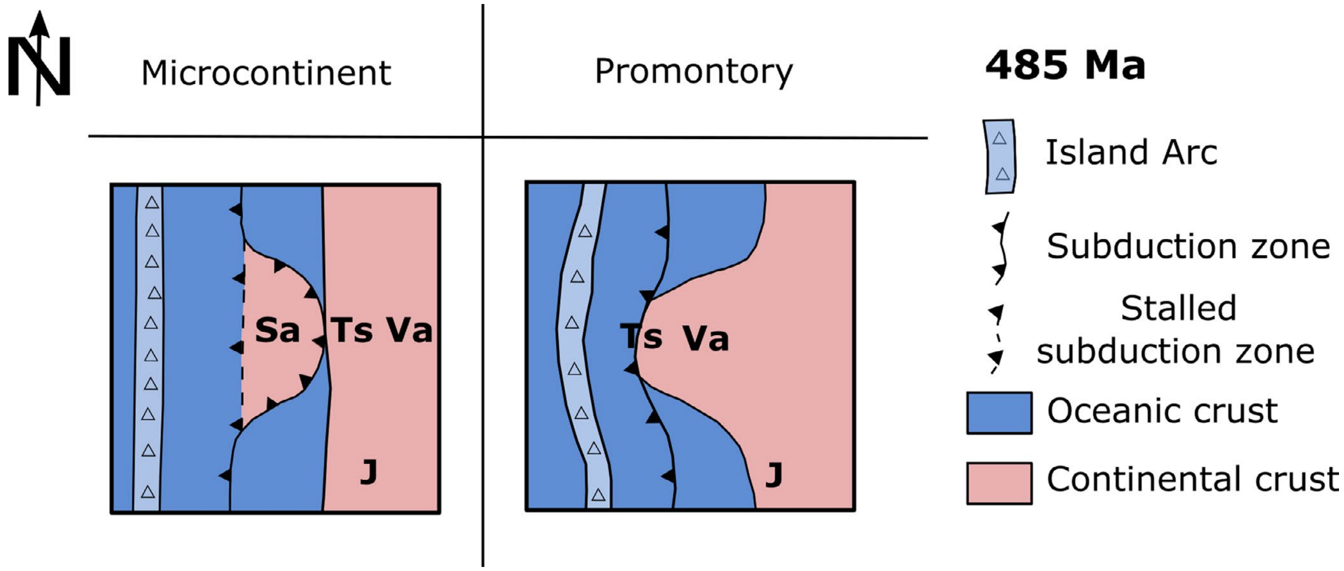

FIGURE 12 Palaeogeographic sketches displaying the different possibilities for the tectonic history of the Seve Nappe Complex, considering either Sarek as a Microcontinent, colliding with the HP unit in Norrbotten before collision in Jämtland or Norrbotten being a promontory of the Baltican continent. Sa = Sarek; Ts = Tsäkkok; Va = Vaimok; J = Jämtland

does not find a straightforward explanation in the traditional framework. One possible explanation would be that the Seve Nappe in Norrbotten represented a promontory in the passive continental marging, leading to a younging of the collision process towards the south (e.g. Barnes et al., 2018; Bukała, Majka, et al., 2020; Petrik et al., 2019; Figure 12).

If, on the other hand, the Andréasson (2020) reconstruction is correct, and the Sarek Lens is in a higher position than both Tsäkkok and Vaimok Lenses, Tsäkkok and Vaimok could still be parts of the ocean–continent transition and continental margin of Baltica, respectively, but Sarek would represent a continental fragment outboard of Baltica. The Sarek Lens is definitely a continental unit because it shows the typical association of metasediments with rifting-related dyke swarms (Svenningsen, 2001). Such a situation has the potential to explain the age difference between Jämtland and Norrbotten eclogites: Sarek represented a microcontinent in the lower plate of the intra-oceanic subduction zone that consumed Iapetus. When the microcontinent collided with the island arc, it was accreted to the upper plate and the subduction boundary jumped to the eastern side of the microcontinent which now formed a promontory of the upper plate. This promontory caused earlier collision in Norrbotten than further south in Jämtland (Figure 12). This scenario could also explain the absence of high-*P* metamorphism in the Sarek Lens because it belonged to the upper plate.

In order to exclude one or the other model, more high-precision dating of prograde HP/UHP metamorphism (preferentially Lu–Hf geochronology on eclogites to ensure comparability) at localities between Norrbotten and Jämtland, and north of Norrbotten is necessary to test this hypothesis, but based on the existent data presented here, we find the model with Sarek being a microcontinent more likely.

6 | CONCLUSIONS

The first Lu–Hf ages for eclogites from the Seve Nappe Complex in Norrbotten were obtained. The ages are interpreted as dating prograde metamorphism during subduction, which happened between 492.3 and 480.0 Ma in the Tsäkkok Nappe, and between 481.6 and 479.2 Ma in the Vaimok Lens. The slight age difference between both nappes is interpreted to be caused by a more outboard origin of the Tsäkkok Nappe when compared to the Vaimok Nappe.

Peak metamorphic conditions of 25–26 kbar at 590–664°C were obtained for the Tsäkkok Nappe by conventional thermobarometry. These conditions are slightly lower than those obtained for the Vaimok Nappe, making it probable that the Vaimok Nappe was subducted deeper.

Ages generally are older in Norrbotten when compared to Jämtland, most probably reflecting a slowly migrating collision of the edge of Baltica with the upper plate. This could be explained by the Seve Nappe in Norrbotten forming a promontory of the Baltican margin. An alternative explanation is that the Norrbotten HP units were subducted under a promontory of the upper plate, formed by an earlier-accreted microcontinent represented by the Sarek Lens.

ACKNOWLEDGEMENTS

We thank Christopher Barnes (AGH University of Science and Technology, Kraków) for providing us with some of the studied samples. Kathrin Fassmer thanks Svenja Trapp and

Matthias Hauke (University of Bonn) for help during Lu–Hf laboratory work. We would also like to thank M. Smit, F. Corfu and A. Kylander-Clark for their reviews which greatly contributed to improving the manuscript. This research was funded by DFG-Grant FR700/18-1 to N. F. and the Slovak Research and Development Agency project APVV-18-0107 to M.J, and partially supported by the National Science Centre (Poland) project 2014/14/ST10/00321 to J. Majka. M.Bukała acknowledges The Polish National Agency for Academic Exchange for the scholarship no. PPN/IWA/2018/1/00046/U/0001. This is contribution no. 64 of the DFG-funded LA-ICP-MS Laboratory at the Institute for Geosciences, University of Bonn, Germany.

ORCID

Kathrin Fassmer https://orcid.org/0000-0002-4598-7457
Michał Bukała https://orcid.org/0000-0001-7045-3150

REFERENCES

Albrecht, L. G. (2000). Early structural and metamorphic evolution of the Scandinavian Caledonides: A study of the eclogite-bearing Seve Nappe Complex at the Arctic Circle, Sweden. PhD thesis, Lund, Sweden.

Andréasson, P.-G. (1986). The Sarektjåkkå Nappe, Seve terranes of the northern Swedish Caledonides. *Geologiska Föreningen I Stockholm Förhandlingar*, *108*(3), 263–266. https://doi.org/10.1080/11035898609454697

Andréasson, P. G. (1994). The Baltoscandian margin in neoproterozoic-early palaeozoic times. Some constraints on terrane derivation and accretion in the Arctic Scandinavian Caledonides. *Tectonophysics*, *231*(1), 1–32.

Andréasson, P.-G., & Albrecht, L. (1995). Derivation of 500 Ma eclogites from the passive margin of Baltica and a note on the tectonometamorphic heterogeneity of eclogite-bearing crust. *Geological Magazine*, *132*(6), 729–738. https://doi.org/10.1017/S001675680001894X

Andréasson, P. G. (2020). The continent-ocean (Seve-Köli) boundary in the Sarek-Padjelanta Mts. revisited: Swedish Caledonides. GFF, 1–14.

Andréasson, P.-G., Svenningsen, O. M., & Albrecht, L. (1998). Dawn of Phanerozoic orogeny in the North Atlantic tract; Evidence from the Seve-Kalak Superterrane, Scandinavian Caledonides. *GFF*, *120*(2), 159–172. https://doi.org/10.1080/11035899801202159

Barnes, C. J., Jeanneret, P., Kullerud, K., Majka, J., Schneider, D., Bukała, M., & Klonowska, I. (2020). Exhumation of the high-pressure Tsäkkok Lens, Swedish Caledonides: Insights from the structural and white mica $^{40}Ar/^{39}Ar$ geochronological record. *Tectonics*, *19*, e2020TC006242.

Barnes, C., Majka, J., Schneider, D., Walczak, K., Bukała, M., Kośmińska, K., & Karlsson, A. (2018). High-spatial resolution dating of monazite and zircon reveals the timing of subduction–exhumation of the Vaimok Lens in the Seve Nappe Complex (Scandinavian Caledonides). *Contributions to Mineralogy and Petrology*, *174*(1), 5.

Baxter, E. F., & Scherer, E. E. (2013). Garnet geochronology: Timekeeper of tectonometamorphic processes. *Elements*, *9*, 433–438. https://doi.org/10.2113/gselements.9.6.433

Brueckner, H. K., & Roermund, H. L. M. V. (2007). Concurrent HP metamorphism on both margins of Iapetus: Ordovician ages for eclogites and garnet pyroxenites from the Seve Nappe Complex, Swedish Caledonides. *Journal of the Geological Society*, *164*(1), 117–128. https://doi.org/10.1144/0016-76492005-139

Brueckner, H. K., & van Roermund, H. L. M. (2004). Dunk tectonics: A multiple subduction/eduction model for the evolution of the Scandinavian Caledonides. *Tectonics*, *23*(2). https://doi.org/10.1029/2003TC001502

Bukała, M., Barnes, C. J., Jeanneret, P., Hidas, K., Mazur, S., Almqvist, B., Kośmińska, K., Klonowska, I., Šurka, J., & Majka, J. (2020). Brittle deformation during eclogitization of early Paleozoic blueschist. *Frontiers in Earth Science*, *8*. https://doi.org/10.3389/feart.2020.594453

Bukała, M., Klonowska, I., Barnes, C., Majka, J., Kośmińska, K., Janák, M., & Luptáková, J. (2018). UHP metamorphism recorded by phengite eclogite from the Caledonides of northern Sweden: P-T path and tectonic implications. *Journal of Metamorphic Geology*, *36*(5), 547–566.

Bukała, M., Majka, J., Walczak, K., Włodek, A., Schmitt, M., & Zagórska, A. (2020). U-Pb zircon dating of migmatitic paragneisses and garnet amphibolite from the high pressure Seve Nappe complex in Kittelfjall, Swedish Caledonides. *Minerals*, *10*(4), 295.

Carswell, D. A., Brueckner, H. K., Cuthbert, S. J., Mehta, K., & O'Brien, P. J. (2003). The timing of stabilisation and the exhumation rate for ultra-high pressure rocks in the Western Gneiss Region of Norway. *Journal of Metamorphic Geology*, *21*(6), 601–612. https://doi.org/10.1046/j.1525-1314.2003.00467.x

Corfu, F., Andersen, T. B., & Gasser, D. (2014). The Scandinavian Caledonides: Main features, conceptual advances and critical questions. In F. Corfu, D. Gasser, & D. M. Chew (Eds.), *New perspectives on the Caledonides of Scandinavia and related areas. Geological Society London Special Publications*, *390*(1), 9–43.

Corfu, F., Ravna, E. J. K., & Kullerud, K. (2003). A Late Ordovician U-Pb age for the Tromsø Nappe eclogites, Uppermost Allochthon of the Scandinavian Caledonides. *Contributions to Mineralogy and Petrology*, *145*(4), 4.

Corfu, F., Roberts, R. J., Torsvik, T. H., Ashwal, L. D., & Ramsay, D. M. (2007). Peri-Gondwanan elements in the Caledonian nappes of Finnmark, northern Norway: Implications for the paleogeographic framework of the Scandinavian Caledonides. *American Journal of Science*, *307*, 434–458. https://doi.org/10.2475/02.2007.05

Cutts, J. A., & Smit, M. A. (2018). Rates of deep continental burial from Lu-Hf garnet chronology and Zr-in-rutile thermometry on (ultra)high-pressure rocks. *Tectonics*, *37*(1), 71–88. https://doi.org/10.1002/2017TC004723

Dallmeyer, R. D. (1988). Polyphase tectonothermal evolution of the Scandinavian Caledonides. *Geological Society, London, Special Publications*, *38*(1), 365–379. https://doi.org/10.1144/GSL.SP.1988.038.01.21

Dallmeyer, R. D., & Gee, D. G. (1986). $^{40}Ar/^{39}Ar$ mineral dates from retrogressed eclogites within the Baltoscandian miogeocline: Implications for a polyphase Caledonian orogenic evolution. *GSA Bulletin*, *97*(1), 26–34. https://doi.org/10.1130/0016-7606(1986)97<26:AMDFRE>2.0.CO;2

Essex, R. M., Gromet, L. P., Andréasson, P.-G., & Albrecht, L. (1997). Early Ordovician U-Pb metamorphic ages of the eclogite-bearing Seve Nappes, Northern Scandinavian Caledonides. *Journal of Metamorphic Geology*, *15*(5), 665–676. https://doi.org/10.1111/j.1525-1314.1997.tb00642.x

Fassmer, K., Klonowska, I., Walczak, K., Andersson, B., Froitzheim, N., Majka, J., Fonseca, R. O. C., Münker, C., Janák, M., & Whitehouse, M. (2017). Middle Ordovician subduction of continental crust in the Scandinavian Caledonides: An example from Tjeliken, Seve Nappe Complex, Sweden. *Contributions to Mineralogy and Petrology*, *172*(103). https://doi.org/10.1007/s00410-017-1420-7

Fassmer, K., Martinet, I., Miladinova, I., Sprung, P., Froitzheim, N., Fonseca, R. O. C., Münker, C., Janák, M., & Kullerud, K. (2020). Lu–Hf geochronology of ultra-high-pressure eclogites from the Tromsø-Nappe, Scandinavian Caledonides: Evidence for rapid subduction and exhumation. *International Journal of Earth Sciences*. https://doi.org/10.1007/s00531-020-01866-0

Fossen, H. (2000). Extensional tectonics in the Caledonides: Synorogenic or postorogenic? *Tectonics*, *19*(2), 213–224. https://doi.org/10.1029/1999TC900066

Froitzheim, N., Miladinova, I., Janák, M., Kullerud, K., Ravna, E. K., Majka, J., Fonseca, R. O. C., Münker, C., & Nagel, T. J. (2016). Devonian subduction and syncollisional exhumation of continental crust in Lofoten, Norway. *Geology*, *44*(3), 223–226. https://doi.org/10.1130/G37545.1

Gale, G. H., & Roberts, D. (1974). Trace element geochemistry of Norwegian Lower Palaeozoic basic volcanics and its tectonic implications. *Earth and Planetary Science Letters*, *22*(4), 380–390. https://doi.org/10.1016/0012-821X(74)90148-4

Ganguly, J., Cheng, W., & Tirone, M. (1996). Thermodynamics of aluminosilicate garnet solid solution: New experimental data, an optimized model, and thermometric applications. *Contributions to Mineralogy and Petrology*, *126*, 137–151. https://doi.org/10.1007/s004100050240

Gee, D. G., Fossen, H., Henriksen, N., & Higgins, A. K. (2008). From the early Paleozoic platforms of Baltica and Laurentia to the Caledonide Orogen of Scandinavia and Greenland. *Episodes*, *31*(1), 44–51. https://doi.org/10.18814/epiiugs/2008/v31i1/007

Gee, D. G., Juhlin, C., Pascal, C., & Robinson, P. (2010). Collisional orogeny in the Scandinavian Caledonides (COSC). *GFF*, *132*(1), 29–44. https://doi.org/10.1080/11035891003759188

Gee, D. G., Kumpulainen, R., Roberts, D., Stephens, M. B., Thon, A., & Zachrisson, E. (1985). Scandinavian Caledonides. Tectonostratigraphic map, Scale 1: 2 M. In D. G. Gee, & B. A. Sturt (Eds.), *The Caledonide Orogen—Scandinavia and related areas*. Wiley.

Gilotti, J. (2013). The realm of ultrahigh-pressure metamorphism. *Elements*, *9*(4), 255–260. https://doi.org/10.2113/gselements.9.4.255

Grimmer, J. C., Glodny, J., Drüppel, K., Greiling, R. O., & Kontny, A. (2015). Early- to mid-Silurian extrusion wedge tectonics in the central Scandinavian Caledonides. *Geology*, *43*(4), 347–350. https://doi.org/10.1130/G36433.1

Gromet, L. P., Sjöström, H., Bergman, S., Claesson, S., Essex, R. M., Andréasson, P. G., & Albrecht, L. (1996). Contrasting ages of metamorphism in the Seve nappes: U-Pb results from the central and northern Swedish Caledonides. *GFF*, *118*, 36–37. https://doi.org/10.1080/11035899609546308

Hacker, B. R., Andersen, T. B., Johnston, S., Kylander-Clark, A. R., Peterman, E. M., Walsh, E. O., & Young, D. (2010). High-temperature deformation during continental-margin subduction & exhumation: The ultrahigh-pressure Western Gneiss Region of Norway. *Tectonophysics*, *480*(1–4), 149–171.

Hacker, B. R., & Gerya, T. V. (2013). Paradigms, new and old, for ultra-high pressure tectonism. *Tectonophysics*, *603*, 79–88. https://doi.org/10.1016/j.tecto.2013.05.026

Hawthorne, F. C., Oberti, R., Harlow, G. E., Maresch, W. V., Martin, R. F., Schumacher, J. C., & Welch, M. D. (2012). Nomenclature of the amphibole supergroup. *American Mineralogist*, *97*(11–12), 2031–2048. https://doi.org/10.2138/am.2012.4276

Holland, T. J. B. (1990). Activities in omphacitic solid solutions: An application of Landau theory to mixtures. *Contributions to Mineralogy and Petrology*, *105*, 446–453.

Holland, T. J. B., & Powell, R. (1998). An internally consistent thermodynamic data set for phases of petrological interest. *Journal of Metamorphic Geology*, *16*, 309–343. https://doi.org/10.1111/j.1525-1314.1998.00140.x

Janák, M., Ravna, E. J. K., & Kullerud, K. (2012). Constraining peak P-T conditions in UHP eclogites: Calculated phase equilibria in kyanite- and phengite-bearing eclogite of the Tromsø Nappe, Norway. *Journal of Metamorphic Geology*, *30*(4), 377–396. https://doi.org/10.1111/j.1525-1314.2011.00971.x

Janák, M., Ravna, E. J. K., Kullerud, K., Yoshida, K., Milovský, R., & Hirajima, T. (2013). Discovery of diamond in the Tromsø Nappe, Scandinavian Caledonides (N. Norway). *Journal of Metamorphic Geology*, *31*(6), 691–703. https://doi.org/10.1111/jmg.12040

Janák, M., van Roermund, H., Majka, J., & Gee, D. (2013). UHP metamorphism recorded by kyanite-bearing eclogite in the Seve Nappe Complex of northern Jämtland, Swedish Caledonides. *Gondwana Research*, *23*(3), 865–879. https://doi.org/10.1016/j.gr.2012.06.012

Jarosewich, E., Nelen, J. A., & Norberg, J. A. (1980). Reference samples for electron microprobe analysis. *Geostandards Newsletter*, *4*(1), 43–47. https://doi.org/10.1111/j.1751-908X.1980.tb00273.x

Jochum, K. P., Weis, U., Stoll, B., Kuzmin, D., Yang, Q., Raczek, I., Jacob, D. E., Stracke, A., Birbaum, K., Frick, D. A., Günther, D., & Enzweiler, J. (2011). Determination of reference values for NIST SRM 610–617 glasses following ISO guidelines. *Geostandards and Geoanalytical Research*, *35*(4), 397–429. https://doi.org/10.1111/j.1751-908X.2011.00120.x

Kirkland, C. L., Daly, J. S., & Whitehouse, M. J. (2006). Granitic magmatism of Grenvillian and late Neoproterozoic age in Finnmark, arctic Norway: Constraining pre-Scandian deformation in the Kalak Nappe Complex. *Precambrian Research*, *145*, 24–52. https://doi.org/10.1016/j.precamres.2005.11.012

Kjøll, H. J., Andersen, T. B., Corfu, F., Labrousse, L., Tegner, C., Abdelmalak, M. M., & Planke, S. (2019). Timing of breakup and thermal evolution of a pre-Caledonian Neoproterozoic exhumed magma-rich rifted margin. *Tectonics*, *38*, 1843–1862. https://doi.org/10.1029/2018TC005375

Klonowska, I., Janák, M., Majka, J., Froitzheim, N., & Kośmińska, K. (2016). Eclogite and garnet pyroxenite from Stor Jougdan, Seve Nappe Complex, Sweden: Implications for UHP metamorphism of allochthons in the Scandinavian Caledonides. *Journal of Metamorphic Geology*, *34*(2), 103–119. https://doi.org/10.1111/jmg.12173

Klonowska, I., Janák, M., Majka, J., Petrík, I., Froitzheim, N., Gee, D. G., & Sasinková, V. (2017). Microdiamond on Åreskutan confirms regional UHP metamorphism in the Seve Nappe Complex of the Scandinavian Caledonides. *Journal of Metamorphic Geology*, *35*(5), 541–564. https://doi.org/10.1111/jmg.12244

Krogh, E. J., Andresen, A., Bryhni, I., Broks, T. M., & Kristensen, S. E. (1990). Eclogites and polyphase P-T cycling in the Caledonian Uppermost Allochthon in Troms, northern Norway. *Journal of Metamorphic Geology*, *8*(3), 289–309. https://doi.org/10.1111/j.1525-1314.1990.tb00474.x

Kullerud, K., & Snilsberg, P. (1987). Origin and tectonometamorphic evolution of the eclogites in the Tsäkkok Lens (Seve Nappes), Southern Norrbotten, Sweden, Unpublished Cand. Scient. thesis. Ph.D. thesis, University of Oslo.

Kullerud, K., Stephens, M. B., & Zachrisson, E. (1990). Pillow lavas as protoliths for eclogites: Evidence from a late Precambrian-Cambrian continental margin, Seve Nappes, Scandinavian Caledonides. *Contributions to Mineralogy and Petrology*, *105*(1), 1–10. https://doi.org/10.1007/BF00320962

Kylander-Clark, A. R. C., Hacker, B. R., Johnson, C. M., Beard, B. L., & Mahlen, N. J. (2009). Slow subduction of a thick ultrahigh-pressure terrane. *Tectonics*, *28*(2). https://doi.org/10.1029/2007TC002251

Kylander-Clark, A. R. C., Hacker, B. R., Johnson, C. M., Beard, B. L., Mahlen, N. J., & Lapen, T. J. (2007). Coupled Lu–Hf and Sm–Nd geochronology constrains prograde and exhumation histories of high- and ultrahigh-pressure eclogites from western Norway. *Chemical Geology*, *242*(1), 137–154. https://doi.org/10.1016/j.chemgeo.2007.03.006

Lagos, M., Scherer, E. E., Tomaschek, F., Münker, C., Keiter, M., Berndt, J., & Ballhaus, C. (2007). High precision Lu–Hf geochronology of Eocene eclogite-facies rocks from Syros, Cyclades, Greece. *Chemical Geology*, *243*(1), 16–35. https://doi.org/10.1016/j.chemgeo.2007.04.008

Lapen, T. J., Johnson, C. M., Baumgartner, L. P., Mahlen, N. J., Beard, B. L., & Amato, J. M. (2003). Burial rates during prograde metamorphism of an ultra-high-pressure terrane: An example from Lago di Cignana, western Alps, Italy. *Earth and Planetary Science Letters*, *215*, 57–72. https://doi.org/10.1016/S0012-821X(03)00455-2

Liou, J. G., Tsujimori, T., Zhang, R. Y., Katayama, I., & Maruyama, S. (2004). Global UHP metamorphism and continental subduction/collision: The Himalayan model. *International Geology Review*, *46*(1), 1–27. https://doi.org/10.2747/0020-6814.46.1.1

Longerich, H. P., Jackson, S. E., & Günther, D. (1996). Inter-laboratory note. Laser ablation inductively coupled plasma mass spectrometric transient signal data acquisition and analyte concentration calculation. *Journal of Analytical Atomic Spectrometry*, *11*(9), 899–904.

Majka, J., Béeri-Shlevin, Y., Gee, D. G., Ladenberger, A., Claesson, S., Konečný, P., & Klonowska, I. (2012). Multiple monazite growth in the Åreskutan migmatites: Evidence for a polymetamorphic Late Ordovician to Late Silurian evolution in the Seve Nappe Complex of the west-central Jämtland, Sweden. *Journal of Geosciences*, *57*, 3–23.

Majka, J., Janák, M., Andersson, B., Klonowska, I., Gee, D. G., Rosén, Å., & Kośmińska, K. (2014). Pressure–temperature estimates on the Tjeliken eclogite: New insights into the (ultra)-high-pressure evolution of the Seve Nappe Complex in the Scandinavian Caledonides. In F. Corfu, D. Gasser, & D. M. Chew (Eds.), *New perspectives on the caledonides of Scandinavia and related areas*. *Geological Society London Special Publications*, *390*, 369–384.

Mørk, M. B. E., Kullerud, K., & Stabel, A. (1988). Sm-Nd dating of Seve eclogites, Norrbotten, Sweden—Evidence for early Caledonian (505 Ma) subduction. *Contributions to Mineralogy and Petrology*, *99*(3), 344–351. https://doi.org/10.1007/BF00375366

Münker, C., Weyer, S., Scherer, E., & Mezger, K. (2001). Separation of high field strength elements (Nb, Ta, Zr, Hf) and Lu from rock samples for MC-ICPMS measurements. *Geochemistry, Geophysics, Geosystems*, *2*(12). https://doi.org/10.1029/2001GC000183

Pedersen, R. B., Bruton, D. L., & Furnes, H. (1992). Ordovician faunas, island arcs and ophiolites in the Scandinavian Caledonides. *Terra Nova*, *4*(2), 217–222. https://doi.org/10.1111/j.1365-3121.1992.tb00475.x

Pedersen, R.-B., Furnes, H., & Dunning, G. (1991). A U/Pb age for the Sulitjelma Gabbro, North Norway: Further evidence for the development of a Caledonian marginal basin in Ashgill-Llandovery time. *Geological Magazine*, *128*(2), 141–153. https://doi.org/10.1017/S0016756800018331

Petrík, I., Janák, M., Klonowska, I., Majka, J., Froitzheim, N., Yoshida, K., Sasinková, V., Konečný, P., & Vaculovič, T. (2019). Monazite behaviour during metamorphic evolution of a diamond-bearing gneiss: A case study from the Seve Nappe Complex, Scandinavian caledonides. *Journal of Petrology*, *60*(9), 1773–1796. https://doi.org/10.1093/petrology/egz051

Ravna, E. J. K. (2000). The garnet-clinopyroxene geothermometer—An updated calibration. *Journal of Metamorphic Geology*, *18*, 211–219.

Ravna, E. J. K., & Roux, M. R. M. (2006). Metamorphic evolution of the Tønsvika Eclogite, Tromsø Nappe—Evidence for a new UHPM province in the Scandinavian Caledonides. *International Geology Review*, *48*(10), 861–881.

Ravna, E. J. K., & Terry, M. P. (2004). Geothermobarometry of UHP and HP eclogites and schists—An evaluation of equilibria among garnet-clinopyroxene-kyanite-phengite-coesite/quartz. *Journal of Metamorphic Geology*, *22*, 579–592. https://doi.org/10.1111/j.1525-1314.2004.00534.x

Roberts, D. (2003). The Scandinavian Caledonides: Event chronology, palaeogeographic settings and likely modern analogues. *Tectonophysics*, *365*, 283–299. https://doi.org/10.1016/S0040-1951(03)00026-X

Roberts, D., & Gee, D. G. (1985). An introduction to the structure of the Scandinavian Caledonides. In D. G. Gee & B. A. Sturt (Eds.), *The Caledonide Orogen—Scandinavia and Related Areas*. Wiley.

Root, D., & Corfu, F. (2012). U-Pb geochronology of two discrete Ordovician high-pressure metamorphic events in the Seve Nappe Complex, Scandinavian Caledonides. *Contributions to Mineralogy and Petrology*, *163*(5), 769–788. https://doi.org/10.1007/s00410-011-0698-0

Root, D. B., Hacker, B. R., Mattinson, J. M., & Wooden, J. L. (2004). Zircon geochronology and ca. 400 Ma exhumation of Norwegian ultrahigh-pressure rocks: An ion microprobe and chemical abrasion study. *Earth and Planetary Science Letters*, *228*(3), 325–341.

Scherer, E. E., Cameron, K. L., & Blichert-Toft, J. (2000). Lu–Hf garnet geochronology: Closure temperature relative to the Sm–Nd system and the effects of trace mineral inclusions. *Geochimica et Cosmochimica Acta*, *64*(19), 3413–3432.

Skora, S., Baumgartner, L. P., Mahlen, N. J., Johnson, C. M., Pilet, S., & Hellebrand, E. (2006). Diffusion-limited REE uptake by eclogite garnets and its consequences for Lu–Hf and Sm–Nd geochronology. *Contributions to Mineralogy and Petrology*, *152*(6), 703–720. https://doi.org/10.1007/s00410-006-0128-x

Smit, M. A., Bröcker, M., Kooijman, E., & Scherer, E. E. (2011). Provenance and exhumation of an exotic eclogite-bearing nappe in the Caledonides: A U–Pb and Rb–Sr study of the Jæren nappe, SW Norway. *Journal of the Geological Society*, *168*(2), 423–439.

Smit, M. A., Scherer, E. E., Bröcker, M., & van Roermund, H. L. M. (2010). Timing of eclogite facies metamorphism in the southernmost Scandinavian Caledonides by Lu–Hf and Sm–Nd geochronology. *Contributions to Mineralogy and Petrology*, *159*(4), 521–539. https://doi.org/10.1007/s00410-009-0440-3

Smit, M. A., Scherer, E. E., & Mezger, K. (2013). Lu–Hf and Sm–Nd garnet geochronology: Chronometric closure and implications for dating petrological processes. *Earth and Planetary Science Letters*, *381*, 222–233.

Soper, N. J. (1994). Neoproterozoic sedimentation on the northeast margin of Laurentia and the opening of Iapetus. *Geological Magazine*, *131*(3), 291–299. https://doi.org/10.1017/S0016756800011067

Stephens, M. B., & Gee, D. G. (1985). A plate tectonic model for the evolution of the eugeoclinal terranes in the central Scandinavian Caledonides. In B. A. Sturt, & D. G. Gee (Eds.), *The Caledonide Orogen: Scandinavia and related areas*. Wiley.

Stephens, M. B., & Gee, D. G. (1989). Terranes and polyphase accretionary history in the Scandinavian Caledonides. In R. D. Dallmeyer (Ed.), *Terranes in the Circum-Atlantic Paleozoic Orogens* (pp. 17–30). *Geological Society of America Special Papers 230*.

Stephens, M. B., & Van Roermund, H. L. (1984). Occurrence of glaucophane and crossite in eclogites of the Seve Nappes, southern Norrbotten Caledonides, Sweden. *Norsk Geologisk Tidsskrift*, *64*(2), 155–163.

Sturt, B. A., Pringle, I., & Ramsay, D. M. (1978). The Finnmarkian phase of the Caledonian orogeny. *Journal of the Geological Society London*, *135*, 597–610. https://doi.org/10.1144/gsjgs.135.6.0597

Svenningsen, O. M. (2001). Onset of seafloor spreading in the Iapetus Ocean at 608 Ma: Precise age of the Sarek Dyke Swarm, northern Swedish Caledonides. *Precambrian Research*, *110*(1), 241–254. https://doi.org/10.1016/S0301-9268(01)00189-9

Van Roermund, H. L. M. (1985). Eclogite from the Seve Nappe, Central Scandinavian Caledonides. In D. G. Gee, & B. A. Sturt (Eds.), *The Caledonide Orogen—Scandinavia and related areas*. Wiley.

Zachrisson, E., & Stephens, M. B. (1984). Mega-structures within the Seve Nappes, southern Norrbotten Caledonides, Sweden. Meddelanden Frå an Stockholms Universitets Geologiska Institution, 255, 241.

How to cite this article: Fassmer K, Froitzheim N, Janák M, et al. Diachronous collision in the Seve Nappe Complex: Evidence from Lu–Hf geochronology of eclogites (Norrbotten, North Sweden). *J Metamorph Geol*. 2021;00:1–24. https://doi.org/10.1111/jmg.12591